Cool Facades and Pavements: Mitigating Heat Stress and Improving Urban Thermal Conditions in Affordable Housing Project – a Case Study in Thailand

WACHARAKORN MANEECHOTE

JIYING LIU [ID]

DARANEE JAREEMIT [ID]

*Author affiliations can be found in the back matter of this article

ABSTRACT

An increase in urban air temperature raises heat stress and mortality risk for city dwellers. This study assessed the potential reductions in air temperature and heat stress through the combined effect of cool façades and floor pavements, in two street canyons in an affordable housing project in Thailand. The air temperature and mean radiant temperatures were simulated for 81 design scenarios where materials with low, medium, and high albedos were used for the walls of buildings, parking areas, and road using ENVI-met v5.0. The risk of exposure to heat stress under extreme conditions was estimated using a heat index equation. The results showed that the avenue canyon (height-to-width ratio, H/W = 0.6) with a low-albedo road surface was hotter than the regular one (H/W = 1.2), due to the larger areas of road pavement and smaller shaded areas. A medium to high albedo for the pavements could reduce the street-level air temperature by up to 2.3°C, but the average mean radiant temperature was raised by 9.3°C. The regular canyon (H/W = 1.2) provided better thermal conditions, and had fewer 'hot spot' areas exposed to heat stress than the avenue canyon. This study explored the benefits of using cool pavements to improve the thermal conditions in areas with limited shade. In addition, this study identified safe outdoor areas not being directly exposed to solar radiation during the hot summer months. These findings could be important for planning safe outdoor activity spaces under extreme heat conditions.

1. INTRODUCTION

The urban heat island (UHI) effect is currently an important topic associated with global climate change, as this problem can affect people's outdoor activities in terms of human comfort and health. Land-surface processes and urban structures such as roads and buildings are considered primary contributors to the UHI effect (Kachenchart et al. 2021; Stone et al. 2010; Zhao et al. 2016; Thammapornpilas 2015). A pavement with a large surface area can absorb more heat from solar radiation and emit it to the surrounding environment, meaning that the air temperature in city areas is typically higher than in rural areas. Excessive heat is trapped and stored in hard-surface urban areas. Exposure to extreme heat increases people's risk of heat exhaustion and heat stroke, which causes heat-related deaths, particularly among lower-income people who spend their time outdoors (Marks & Cornell 2023). It is also crucial to take extra precautions when the weather is hot and humid, especially for certain groups such as the elderly, young children, and pregnant women, who are more sensitive to heat than others (National Weather Service 2023).

About 1,000 heat-related deaths are reported each year globally, and European countries have the highest mortality risk from heatwaves (Vicedo-Cabrera et al. 2021). The air temperature of Thailand is increasing by 0.15℃ per decade, with a total rise over recent years of 40.5% (Kachenchart et al. 2021). Arifwidodo and Chandrasiri (2015) revealed that the UHI intensity for Bangkok city was approximately 6–7℃, and was worse than the other major cities in Asia Pacific. High urban air temperatures cause discomfort and pose risks to human health by increasing the risk of heat stroke, dehydration, and heat-related illnesses. About 243 Thai people have died from heat waves since 2015, according to the Department of Disease Control of Thailand (Department of Disease Control 2022), and between 2,500 and 3,000 people are hospitalized each year due to heat-related illness. In addition to its effect on human comfort and health, a rise in air temperature could increase building cooling loads (Salvati et al. 2022; Jareemit & Canyookt 2020; Nazarian et al. 2019). Urban heat islands are becoming a pressing issue as cities grow and expand, and many countries are now taking action and implementing solutions to reduce the amounts of heat trapped in urban areas. This can not only improve the comfort level of residents but also help to mitigate the impact of climate change.

Although reducing high urban air temperatures is essential for human comfort and health, this poses a significant challenge to city planners and architects. Various heat mitigation strategies have been employed, such as green roofs and vertical green walls, cool pavements, and planting more trees (Oke et al. 2017; Leetongin et al., 2022; Mohammad et al., 2021). Shading is an important design parameter for improving outdoor conditions in hot and humid climates, as it promotes outdoor livability, encourages activities, and prevents surface pavements from becoming excessively hot due to direct exposure to solar heating. This, in turn, reduces heat absorption (Rahman et al. 2021; Fang et al. 2023) and makes the outdoor environment much more comfortable. Previous studies (Srivanit & Jareemit 2020; Kotopouleas et al. 2021; Tochaiwat et al., 2023) have explored the benefits of shading in hot-humid climates through increasing the ratio of building height to street width (H/W), planting trees along streets, and using varying building orientations. It has been found that the impact of cool pavements in terms of a reduction in air temperature in shaded areas is not significant due to the shade protect surface pavement directly exposed to the solar heat resulting in less heat absorption (Schrijvers et al. 2016; Nasrollahi et al. 2020; Zhang et al. 2021).

In areas with limited shade, and particularly on streets oriented along the E-W direction and exposed to solar radiation throughout the day, it is important to consider the urban surface albedo as a significant factor in mitigating UHI and thermal stress, as noted by Srivanit and Jareemit (2020), Zhang et al. (2021), and Takebayashi and Moriyama (2012b). Increasing the surface albedo can prevent excessive heat absorption, and can promote a more comfortable outdoor environment (Greater London Authority 2006; Oke et al.2017; Ford & Ford 2000; Erell et al. 2014; Mohammad et al. 2021). Albedo, or solar reflectivity, is the ratio of reflected solar radiation to the incident solar radiation at the surface, and its value ranges from zero to one. A material with an albedo of zero absorbs all solar radiation, while one with an albedo of one perfectly reflects sunlight. In urban design, it is typically assumed that a pavement with a high albedo (high reflectance) can reflect more sunlight to the sky.

Studies of the effect of high-albedo materials on UHI reduction have been carried out at various scales, including street canyons, building clusters, neighborhoods, and cities (Lopez-Cabeza et al. 2022; Taleghani 2018; Mohammad et al. 2021; Anand & Sailor 2022). It has been reported that the use of paving surfaces made of more highly reflective materials can help to reduce extreme heat during the day and indirect night cooling (Probst et al. 2022). The temperature reduction can vary from 0.2–0.5℃, which seems small but which may help a little in extreme heat (Lopez-Cabeza et al. 2022; Sen et al. 2019). Several works have compared the temperature reduction due to a single surface effect, and a few have tried to increase temperature reduction by applying high-reflectance materials to building façades (Salvati et al. 2022; Zhang et al. 2022; Yang and Li 2015). The combined effect

of cool materials on the walls, pavements, and roofs was found to provide the most significant temperature reduction of about 0.8–1.1°C, which was greater than using only a single surface (Sen et al. 2019; Salvati et al. 2022; Lopez-Cabeza et al. 2022; Schrijvers et al. 2016).

The effect of cooler pavements on air temperature reductions may also vary depending on the canyon geometry and sky view factor (Salvati et al. 2022; Choi et al. 2018). A street canyon with a higher H/W ratio provides more surrounding shade, while a greater urban surface area increases the reflected radiation from walls and paving surfaces (Salvati et al. 2022). The use of highly reflective surfaces can have a negative effect on outdoor thermal comfort in the summer, as it can raise the mean radiant temperature due to high reflected solar radiation and diffuse radiation from adjacent building façade and floor surfaces (Falasca et al. 2019; Lopez-Cabeza et al. 2022). It is therefore necessary to consider these factors when designing outdoor spaces.

UHI intensity is used as a measure of the differences in temperature between urban and suburban areas. Previous studies of UHI have typically investigated three heights, relating to the surface UHI (SUHI), the canopy layer UHI (CLUHI), and the boundary layer UHI (BLUHI) (Parsaee et al. 2019). The CLUHI measures the air temperature difference at a distance of 2 m above a surface, and this metric has the greatest impact on human activities. The temperature measurements used for the SUHI and BLUHI are taken at the surface and 2 km above the surface (atmospheric boundary layer), respectively. The UHI effect varies depending on the geography of the land and the urban geometry. Various simulation CFD tools have been used to evaluate the microclimate in urban environments, with different levels of complexity (Lopez-Cabeza et al. 2022; Acharya et al. 2021; Taleghani et al. 2015; Zheng et al. 2022). One of these tools is ENVI-met software, which applies fluid mechanics and thermodynamics principles to model the interactions between the ground, vegetation, buildings, and atmosphere at different urban scales (Bruse & Fleer 1998). This tool can enable a better understanding of urban climate issues.

Previous research has focused on the replacement of single cooling surfaces such as road pavements or building facades to lower air temperatures, and there is limited research on the potential benefits of using variable albedos on different surfaces, such as building facades, parking areas, and roads, in two different-sized street canyons. In this study, we therefore investigated the possible reductions in air temperature and heat stress in E-W street canyons with few shading structures by implementing a range of different surface designs for floor pavements and building facades. One aim of the study was to gain a better understanding of how cool surfaces can significantly improve thermal conditions in such canyons while reducing the risk of heat stress. In this study, microclimate simulations were carried out with ENVI-met v.5.0 to analyze the hourly thermal conditions at the street level and to calculate the heat stress levels, in order to assess the exposure risk. The findings will help in the design of solutions to mitigate the effects of UHI and to reduce the risk of heat stress-related illnesses in E-W-oriented streets.

2. SITE LOCATION AND CASE STUDY

A multi-residential community of low-income people was selected as a case study. The National Housing Authority (NHA) of Thailand operates more than 4,451,540 units of affordable housing, and housing units in residential apartment buildings currently account for 12% of the total public housing units (Wongbumru & Dewancker 2014). This area is densely populated, and needs more public space. In addition, the nearby buildings provide very little shade, which poses a challenge in terms of improving thermal conditions. People undertaking outdoor activities in this area have a high risk of exposure to extreme heat. The study first classified building layouts from 23 of the NHA's housing projects around Bangkok and suburban areas to select a site. The most common building layout (representing about 38% of the total number of buildings), on streets oriented in the E-W direction (with the worst heat conditions), was then selected as a representative study area. The site was located to the west of Bangkok city (13°45'33.4"N 100°43'36.6" E) (see Figure 1), and had dimensions of 300 × 300 m. This housing project has a main road separating the north and south building clusters and a small network of roads running between the buildings. A large green space with undeveloped land is located to the south of the housing project.

Street canyon is categorized by its dimensions using building height to street width (H/W) ratios into avenue (H/W < 0.5), regular (H/W ≈ 1.0), and deep (H/W > 2.0) canyons. Another classification is based on building length to building height (L/H) ratios, dividing into short (L/H < 3), medium (L/H = 5), and long (L/H > 7) canyons (Afiq et al., 2012). The characteristics of the street canyon and building design in this housing project were as follows. Each building was 17.6 m in width and 94.5 m in length, with a height of five stories (23m). The width of the wider canyon (B) was 40 m (H/W = 1.2), categorized as regular canyon, and that of the narrower canyon (A) was 20 m (H/W = 0.6), which is the category of avenue canyon. Figure 2 shows the cross-sections and dimensions of street canyons A and B. The widths of the roads in canyons A and B were 7 m
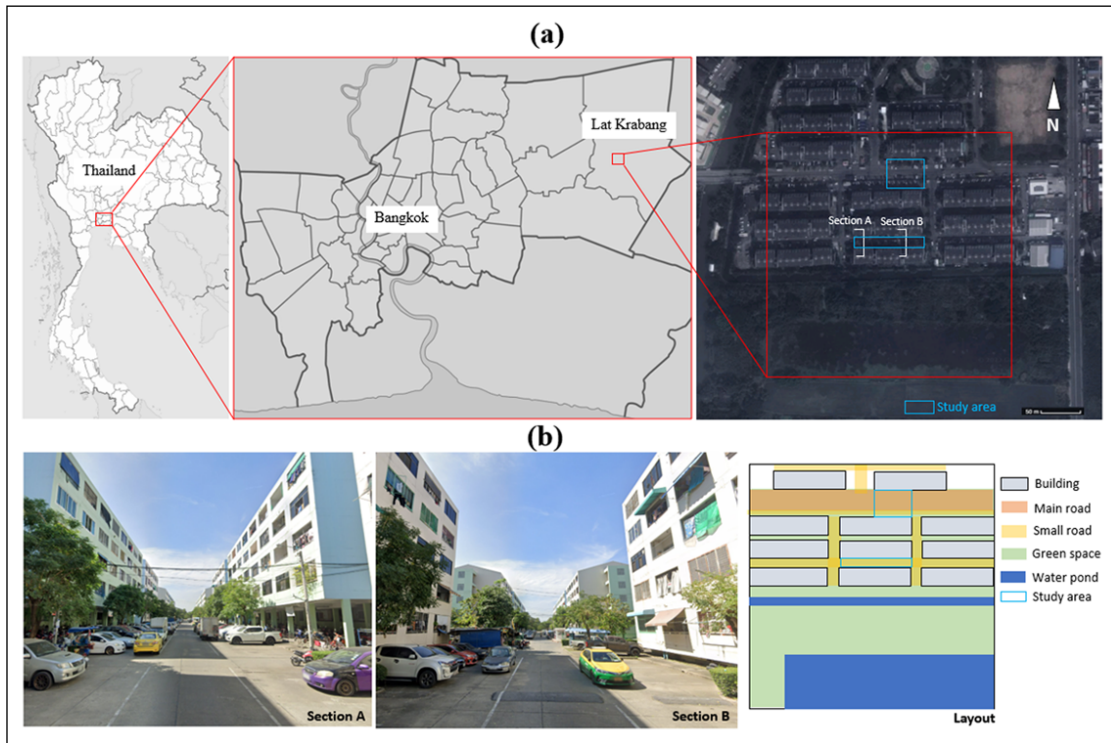
Figure 1 Site location **(a)** and street canyon characteristics **(b)** of the building layout and surrounding environment.
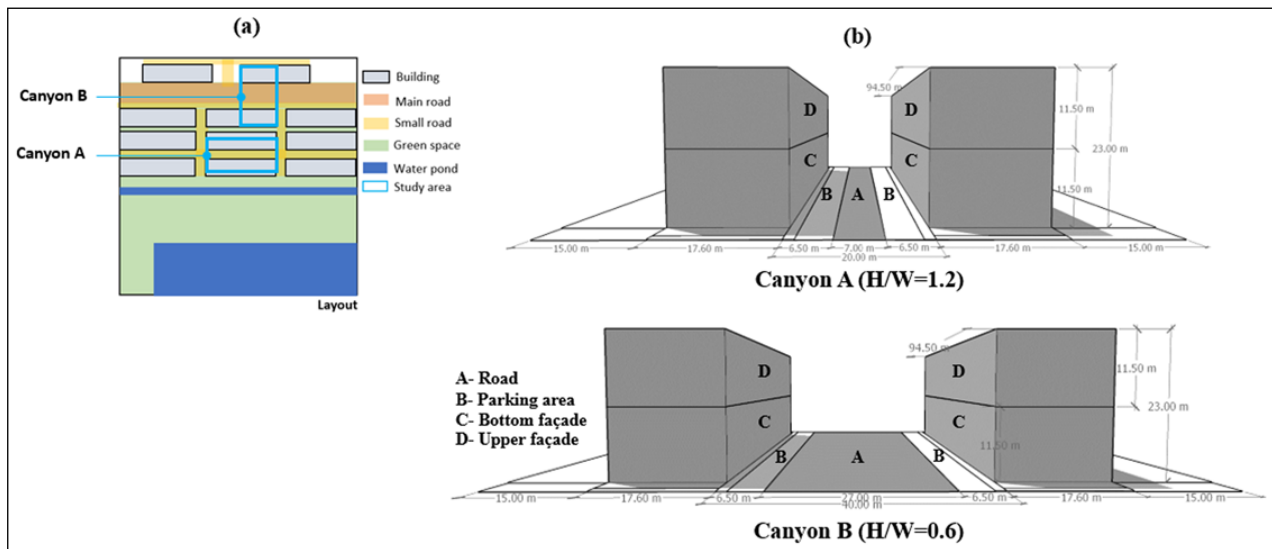

Figure 2 Building layout **(a)** and cross-sections and dimensions of street canyons A and B **(b)**.

and 27 m, respectively, while the width of the vehicle parking lanes along the roadside was 6.5 m for both. Due to the limited availability of parking lots, some cars were parked in the vehicle lanes during the night and in the morning, but most leave during the day. There were three or four trees in each street canyon. However, the effect of car parking and tree planting were not considered in this study because we aimed to assess the cooling effect influenced by surface albedos. However, their effects should be considered in a real situation.

3. RESEARCH METHODOLOGY

The study use simulation method to perform outdoor thermal conditions in two street canyons located in the study site. The field measurement of air temperature and calculated mean radiant temperature were conducted to compared with the simulation results. Then we assessed the potential use of cool surfaces applied in the canyon surface to improve outdoor air temperature and reduce heat stress risk for outdoor living. The study's framework shown in Figure 3.

3.1 DESIGN SCENARIOS

We evaluated the influence on cooling performance of changing the surface materials for pavements and building façades. Varying designs of high, medium, and low reflective materials were applied to the road surface, building facades, and parking areas (including pedestrian paths). The selected values for the albedo were based on typical materials used for paving surfaces and wall construction in Thailand, and were drawn from a material database provided with the ENVI-met model. The details are given in Table 1. The building façade was separated into a lower part (0–11.5 m) and an upper part (11.5–23 m), as previous authors have reported that the use of a reflective material for the lower part of a wall significantly affects human thermal comfort (Salvati et al. 2022). Finally, 81 design combinations of canyon surface albedos, including a base case (C81), were generated to perform microclimate simulations, as shown in Figure 4. Each case has a 4-letter code; for example, HHHH, that identify the surface material applied to the upper façade, lower façade, parking area, and road, respectively.

3.2 SETTINGS FOR ENVI-MET SIMULATION MODELING

An investigation of the thermal performance of all design combinations was carried out using the ENVI-met (Bruse & Fleer 1998) microclimate model. The ENVI-met model is a valuable tool for accurately assessing microclimate conditions at various scales, from simple to complex urban environments (Salvati et al. 2022; Alssad et al. 2022; Crank et al. 2020; Maggiotto et al. 2014). This three-dimensional software was developed based on fluid dynamics and thermodynamics principles, and offers an algorithm for calculating the radiative flux emitted from plants and materials and their effects on the radiative conditions (Bruse 2004). The input data required for the ENVI-met model are presented in Table 2, and include the study location, domain size, duration of the simulation, and meteorological conditions.

Figure 5 shows the domain size, nesting grid, and building layout in ENVI-met software. The number of nested grids around the main 3D model was eight, which was sufficient for numerical stability. The date modeled in the simulation was June 20, 2022; a summer day was chosen for analysis because this imposes the worst heat conditions, due to a lack of surrounding shade. A change in the albedos of the pavement and buildings could therefore significantly affect the temperature reduction in the street space. To reflect the meteorological conditions, weather data including the hourly air temperatures, relative humidity, wind speed and direction were drawn from five-year
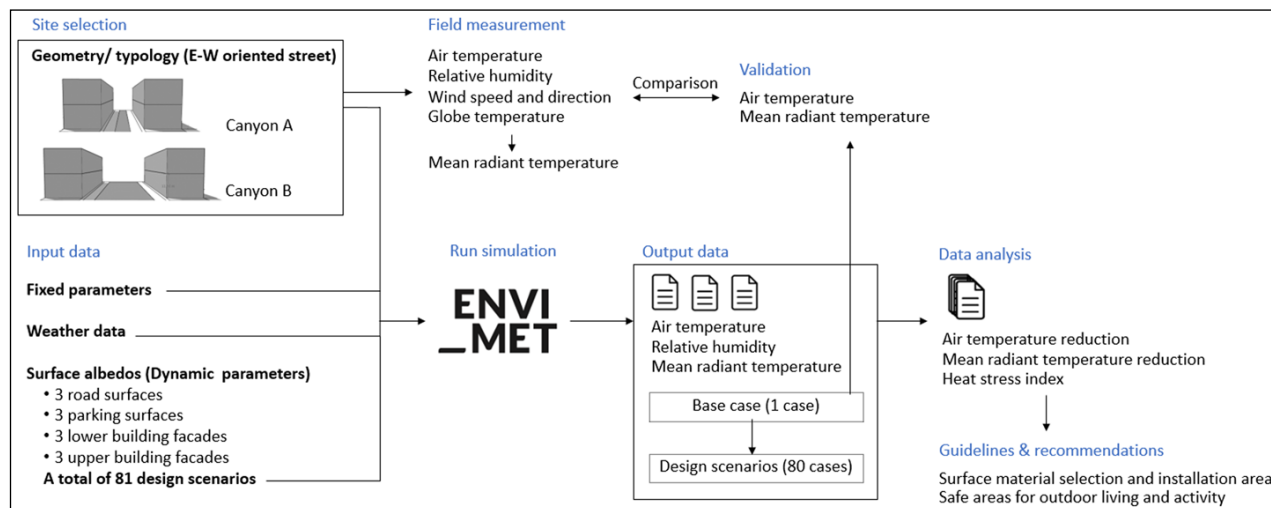

Figure 3 Research workflow on the assessment of outdoor microclimate and heat stress levels from difference design scenarios.

SURFACE TYPE	LOCATION (SEE FIGURE 2)	LOW REFLECTIVE MATERIAL (ALBEDO VALUE)	MEDIUM REFLECTIVE MATERIAL (ALBEDO VALUE)	HIGH REFLECTIVE MATERIAL (ALBEDO VALUE)
Road	A	Black concrete (0.3)	Gray concrete (0.5)	Bright concrete (0.8)
Parking area	B			
Lower façade	C	Dark concrete brick (0.1)	Lightweight brick wall (0.4)	Bright concrete brick (0.7)
Upper façade	D			

Table 1 Types of flooring, wall materials, and albedo values used for pavements and building façades.

Design scenario	Upper façade	Lower façade	Parking area	Road	Design scenario	Upper façade	Lower façade	Parking area	Road
C01	H	H	H	H	C41	M	M	M	M
C02	H	H	H	M	C42	M	M	M	L
C03	H	H	H	L	C43	M	M	L	H
C04	H	H	M	H	C44	M	M	L	M
C05	H	H	M	M	C45	M	M	L	L
C06	H	H	M	L	C46	M	L	H	H
C07	H	H	L	H	C47	M	L	H	M
C08	H	H	L	M	C48	M	L	H	L
C09	H	H	L	L	C49	M	L	M	H
C10	H	M	H	H	C50	M	L	M	M
C11	H	M	H	M	C51	M	L	M	L
C12	H	M	H	L	C52	M	L	L	H
C13	H	M	M	H	C53	M	L	L	M
C14	H	M	M	M	C54	M	L	L	L
C15	H	M	M	L	C55	L	H	H	H
C16	H	M	L	H	C56	L	H	H	M
C17	H	M	L	M	C57	L	H	H	L
C18	H	M	L	L	C58	L	H	M	H
C19	H	L	H	H	C59	L	H	M	M
C20	H	L	H	M	C60	L	H	M	L
C21	H	L	H	L	C61	L	H	L	H
C22	H	L	M	H	C62	L	H	L	M
C23	H	L	M	M	C63	L	H	L	L
C24	H	L	M	L	C64	L	M	H	H
C25	H	L	L	H	C65	L	M	H	M
C26	H	L	L	M	C66	L	M	H	L
C27	H	L	L	L	C67	L	M	M	H
C28	M	H	H	H	C68	L	M	M	M
C29	M	H	H	M	C69	L	M	M	L
C30	M	H	H	L	C70	L	M	L	H
C31	M	H	M	H	C71	L	M	L	M
C32	M	H	M	M	C72	L	M	L	L
C33	M	H	M	L	C73	L	L	H	H
C34	M	H	L	H	C74	L	L	H	M
C35	M	H	L	M	C75	L	L	H	L
C36	M	H	L	L	C76	L	L	M	H
C37	M	M	H	H	C77	L	L	M	M
C38	M	M	H	M	C78	L	L	M	L
C39	M	M	H	L	C79	L	L	L	H
C40	M	M	M	H	C80	L	L	L	M
					C81	L	L	L	L

Figure 4 A total of 81 design scenarios used to perform microclimate simulation. H, M, and L represent to high, medium, and low albedo values.

average data for June 2018–2022, obtained from a nearby weather station (Suvarnabhumi Airport, 13.69°N, 100.75°E). The boundary meteorological conditions used a simple forcing mode, which required hourly average air temperatures and relative humidities over a 24-hour. Figure 6 shows the hourly air temperature and relative humidity data that were input to the model. The wind speed and direction remained constant throughout the simulation. The simulation was performed for 23 hours.

3.3 ASSESSMENT OF HEAT STRESS LEVEL IN STREET CANYON

Heat stress and thermal comfort indices are important in designing environments, which widely used for assessing thermal conditions in outdoor environment (Erell et al., 2014; Arifwidodo and Chandrasiri, 2020; Jareemit and Srivanit, 2022; Falasca et al., 2019). However, they serve different purposes. Heat stress refers to the body's inability to regulate its internal temperature when the

body absorbs more heat that can cause heat-related illnesses such as heat exhaustion and heat stroke. On the other hand, thermal comfort is the individual's mental satisfaction with their surrounding thermal environment. Therefore, the study selected the heat stress index to directly assess the risk of heat stress level for preventing harm in extreme condition for outdoor living in low-rise residential housing. The National Weather Service provides several heat stress indicators, including the heat index (HI), wet bulb globe temperature (WBGT), and the heat risk category. These tools have unique strengths and limitations in terms of their implementation (US Department of Commerce 2023). The HI is most commonly used, as it is a well-known and easily understandable assessment tool. It was developed by Steadman in collaboration with state Public Health Departments (Steadman 1979). This index is the result of extensive biometeorological studies involving several parameters; however, it has limited value when the

LOCATION	VALUE
Site location	Lat Krabang, Bangkok
Latitude	13.69°N
Longitude	100.75°E
Model domain settings	
Grid size (number of grid cells)	1 × 1 × 2 m (100 × 100 × 25)
Nested grids	8
Soil profiles in nested grids	Loamy soil (LO)
Date and duration of simulation	
Simulation date	June 20, 2022
Start time	23 h from 1 am to 11 pm
Meteorological conditions	
Wind speed measured at 10 m height (prevailing wind direction)	3.7 m/s (south)
Roughness length at the measurement site	0.01 m (default value)
Initial air temperature	26–36°C
Initial relative humidity	39–89%
Specific humidity at 2500 m height	7 g/kg (default value)

Table 2 Input parameters for the ENVI-met model.

this formula is used, the air temperature in degrees Celsius (°C) needs to be converted to Fahrenheit (F). This equation was developed from multiple regression analyses with an error of 1.3 F (Rothfusz 1990). Risk assessments based on the heat stress index or human discomfort index are classified into four levels of warning, as presented in Table 3.

$$
\begin{aligned}
\text{Heat stress index}(^{o}F) \\
= -42.379 + (2.04901523\,T_{air}) + (10.1433127\,RH) \\
- (0.22475541\,T_{air}RH) - (6.83783 \times 10^{-3}\,T_{air}^{2}) \\
- (5.481717 \times 10^{-3}\,T_{air}^{2}RH) + (8.5282 \times 10^{-4}\,T_{air}RH^{2}) \\
- (1.99 \times 10^{-6}\,T_{air}^{2}RH^{2})
\end{aligned} \tag{1}
$$

3.4. FIELD EXPERIMENTS AND MODEL VALIDATION

To optimize the simulation time and assess the accuracy of the model settings, the study first compared the simulation results for the air temperature, relative humidity, and mean radiant temperature for three different grid sizes: a finer grid (1 × 1 × 2 m with 250,000 grid cells), a fine grid (2 × 2 × 2 m with 62,500 grid cells) and a coarse grid (3 × 3 × 2 m with 27,777 grid cells) with data measured in the field. To collect the field data, a Krestel weather and environment meter was used to conduct hourly measurements of air temperature, relative humidity, globe temperature, wind speed, and wind direction between 1 p.m. and 5 p.m. on June 20,
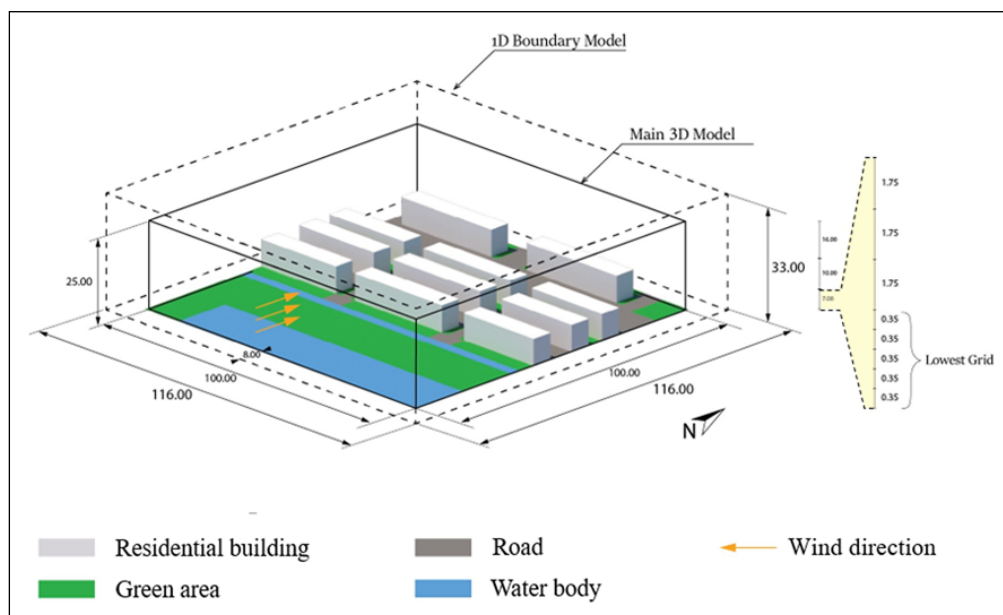

Figure 5 Domain size and site model in ENVI-met software.

conditions involve low humidity, and may give a high uncertainty for the heat impacts on active individuals. A simplified model can be used to calculate HI, as shown in Equation (1), which includes two significant parameters: air temperature (T_{air}) and relative humidity (RH). When

2022. The instrument was placed at a height of 1.4 m above the ground at the center of canyons A and B, as shown in Figure 7. From the field-measured data, the mean radiant temperature was calculated from air temperature (T_{air}), globe temperature (T_{g}), and wind
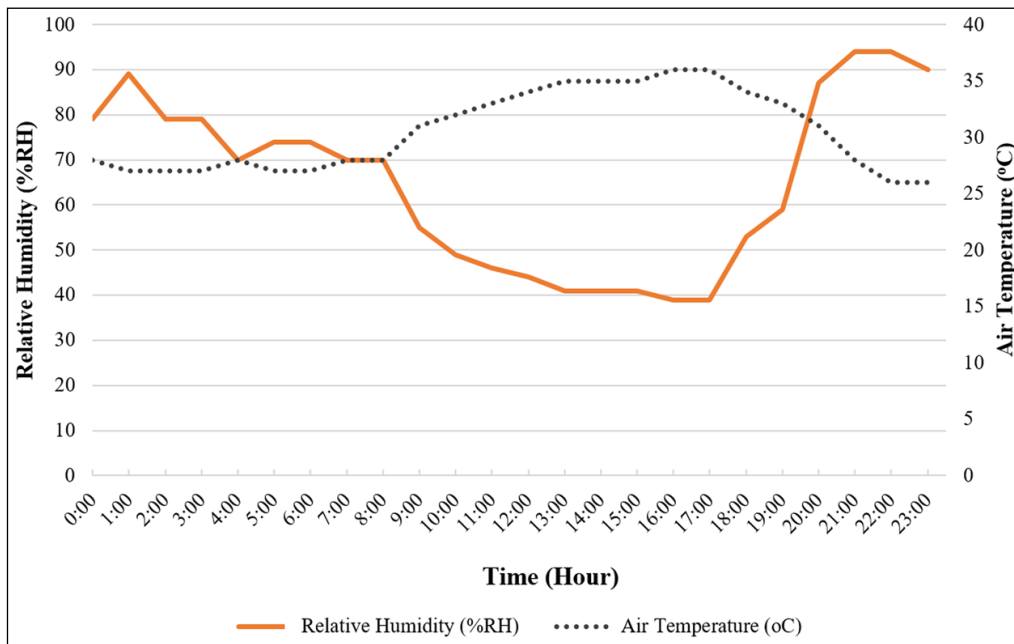
Figure 6 Average hourly air temperatures and relative humidities for June 2018–2022.

speed (V_a), according to ISO 7726, as shown in Equation (2). In this study, the emissivity (ε) was 0.95 and globe diameter was 0.05 m.

$$T_{mrt} = \left[(T_g + 273.15)^4 + \frac{1.335 \times 10^8 V_a^{0.71}}{\varepsilon D^{0.4}} (T_g - T_{air}) \right]^{1/4} - 273.15 \quad (2)$$

The hourly simulation results and measured data were plotted for comparison (see Figure 8). The average percentage error for the coarse and fine grids compared to the measured data was relatively high (with an average of 15–28%), while the error between the finer grid and the measured data was lower (5–15%). Consequently, the best option for this study, which provided acceptable errors, was the finer grid of size 1 × 1 × 2 m.

HEAT STRESS INDEX		HEALTH EFFECT
°C	**°F**	
27–32	80–90	Caution: fatigue possible with prolonged exposure and activity; continuing activity could result in heat cramps
32–41	90–105	Extreme caution: heat cramps and heat exhaustion possible; continuing activity could result in heat stroke
41–54	105–130	Danger: heat cramps and heat exhaustion likely; heat stroke probable with continued activity
Over 54	Over 130	Extreme danger: imminent heat stroke

Table 3 Level of heat stress and effects on human health (US Department of Commerce 2023).

Note: These data were adapted from the US NOAA National Weather Service Heat Index.

Next, to validate the model, the simulation results obtained for the finer grid setting were compared with measured data using three statistical models: R^2, CV(RMSE) (Equation 3), and NMBE (Equation 4). It can be seen from Table 4 that the errors in the air temperature and mean radiant temperature were within the acceptable range for the hourly criteria defined in ASHRAE Guideline 14 (Ruiz & Bandera 2017), even though the errors for relative humidity were higher than the field data. Finally, we note that the finer grid size was used, as it could provide reliable results.

$$CV(RMSE) = \frac{1}{m} \cdot \sqrt{\frac{\sum_{i-1}^n (m_i - s_i)^2}{n-p}} \times 100 \, (\%) \quad (3)$$

$$NMBE = \frac{1}{m} \cdot \frac{\sum_{i-1}^n (m_i - s_i)^2}{n-p} \times 100 \, (\%) \quad (4)$$

4. RESULTS

This section presents the key findings related to thermal conditions and the influence of the design factors on the areas with exposure to heat stress risk.

4.1 HOURLY DATA ON AIR TEMPERATURE, RELATIVE HUMIDITY, AND MEAN RADIANT TEMPERATURE IN STREET CANYONS

Figure 9 presents the hourly air temperature and mean radiant temperature profiles for some selected scenarios with low- and high-albedo paving materials. The average air temperature and mean radiant temperature at night were 26.8°C and 18.5°C, respectively; these increased after 6 a.m. and dropped after 2 p.m., corresponding to the solar radiation profile.
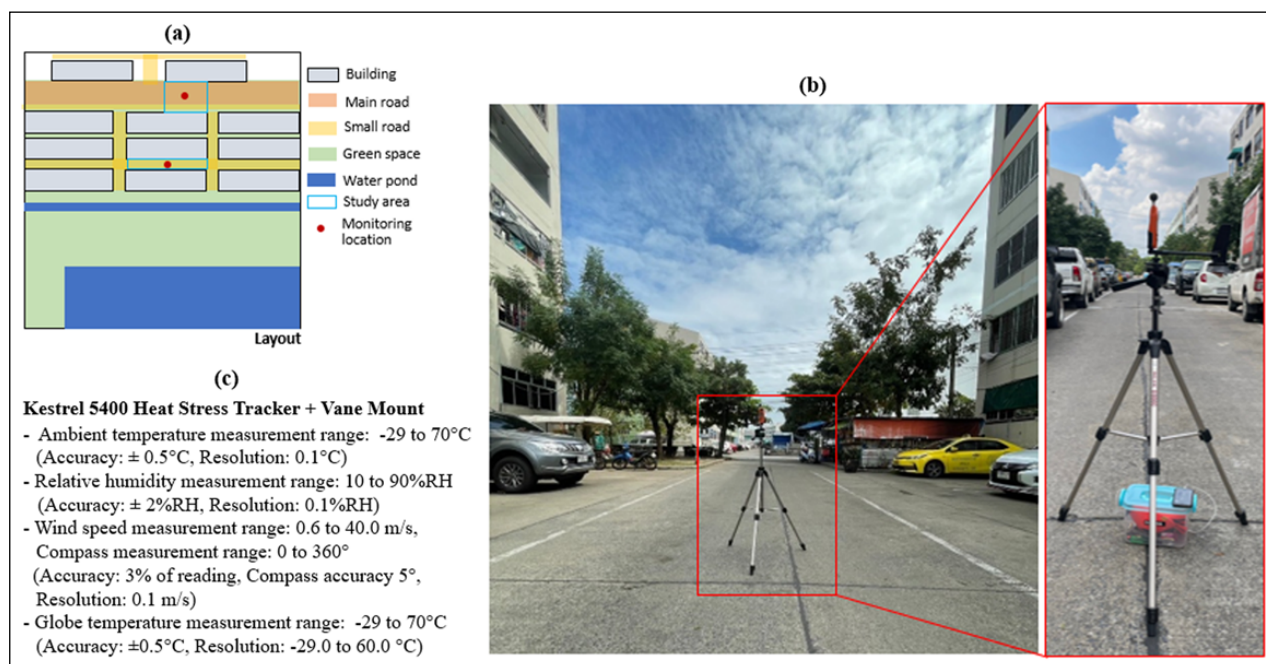
Figure 7 Location of the field monitoring station **(a)** and instrument setting in the street canyons **(b)**, and instrument information **(c)**.

The study found that the street canyon with cool surfaces (high albedo) typically had a lower air temperature during the daytime (with values ranging from 27°C to 35°C) compared to those paved with low-albedo materials (with values ranging from 26°C to 37°C). The relative humidity and mean radiant temperature profiles also showed that the designs with low albedos had lower levels for these parameters than those with high albedos. The most significant change in the air temperature and mean radiant temperature was found at 2 p.m, whereas during the night, the changes were relatively small.

Figure 10 (left) shows the average air temperature and mean radiant temperature at the pedestrian level in canyons A and B at 2 p.m. The air temperatures in canyon A were ranked from low to high. High-albedo surfaces (C01, HHHH) had the lowest air temperature (35.2°C), while those in the low-albedo canyon (C81, LLLL) had the highest (37.3°C). Figure 10 (right) shows the rankings of the predicted mean radiant temperatures, ranging from 60.7°C to 68.6°C. An unexpected finding was that the mean radiant temperature ranking was not correlated with the air temperature; for example, C54 (MLLL) was the second rank of high mean radiant temperatures but not the for the air temperatures. Figure 11 presents the box plot distribution of air temperature and mean radiant temperature in canyons A and B. Overall the air temperature in canyon A lower than canyon B, while the mean radiant temperature in canyon B has the same distribution range as those of canyon A, but the average value was slightly higher. Interestingly, the air temperatures in canyon B distinctly separated into 3 groups when the road was paved with high, medium, and low albedos, respectively, while canyon A had heterogeneous distribution.

Figures 12 and 13 present air temperature and mean radiant temperature contours in the studied site for C01 (HHHH) and C81 (LLLL). The distribution of air temperature, relative humidity, and mean radiant temperature across the section of street canyons A and B when applied different surface materials were assessed and compared.

Figure 14 shows the average air temperatures at a height of 1.4 m above the ground across canyons A and B in eight selected scenarios. There was a significant difference in air temperature (about 1–2°C) when the road and parking surfaces were made of materials with low and high albedos. The use of high-albedo materials on these surfaces improved the air temperature in canyon B more than for canyon A. The temperatures on the right side were lower than those on the left, due to shading from buildings. In canyon A, the difference in air temperature between the design scenarios was consistent across the canyon; however, in canyon B, significant differences in air temperature typically occurred near the building façades, and their magnitudes gradually declined far from the building façades. From Figure 15, it can be seen that the relative humidity profile showed opposite behavior to the air temperature profile. The mean radiant temperature is shown in Figure 16, and we can observe that the temperature difference between the scenarios was consistent across the canyon, except for a significant drop on the right-hand side due to shade from buildings.

4.2 POTENTIAL FOR TEMPERATURE REDUCTION AND SIGNIFICANT DESIGN FACTORS

Compared to the worst scenario (C81, LLLL), the combined effects of cool-surface conditions (C01,
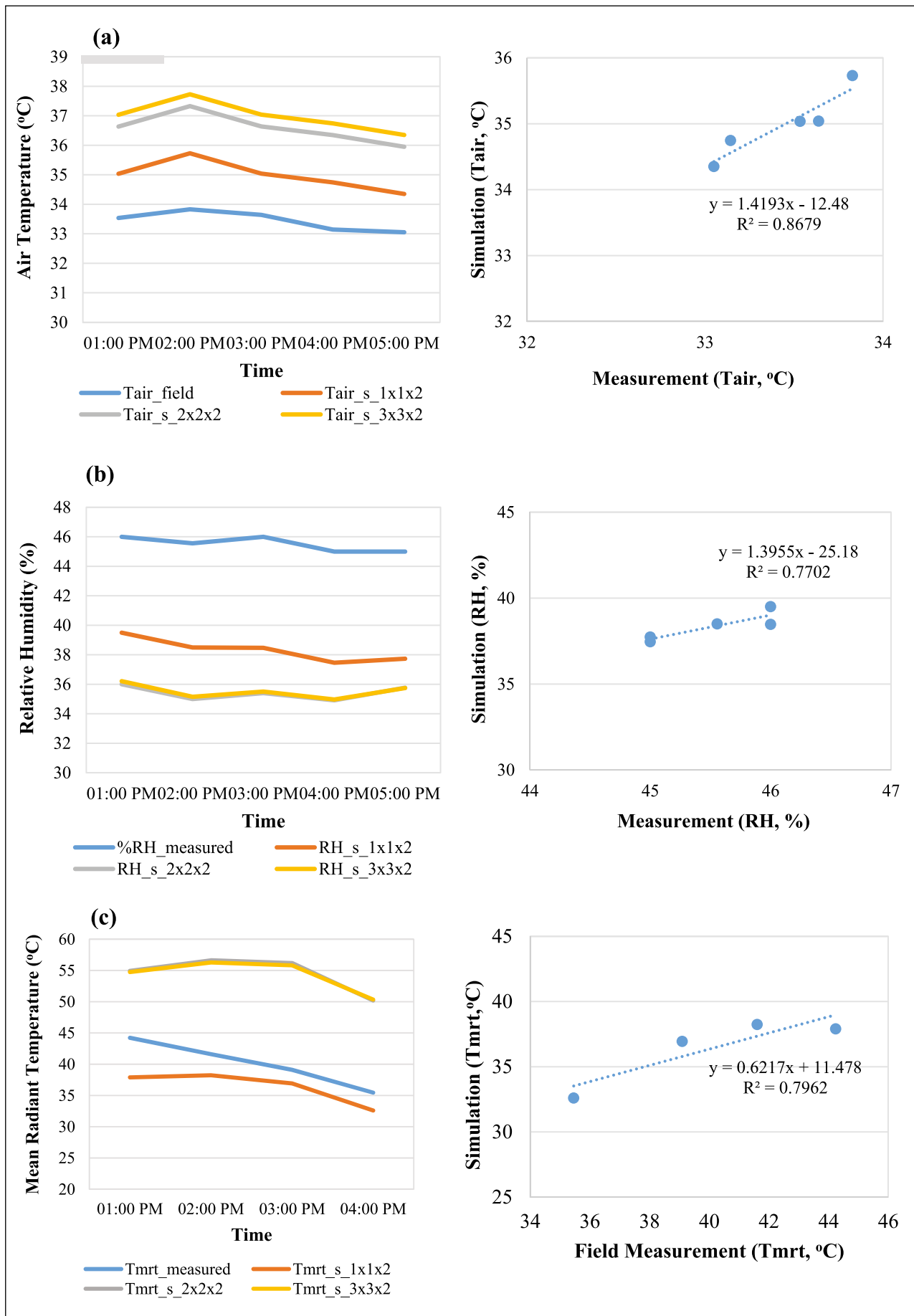
Figure 8 Comparisons between field measured data and simulation results of air temperature **(a)**, relative humidity **(b)**, and mean radiant temperature **(c)**.

STATISTICAL MODEL	RELATIVE ERROR IN T_{air}	RELATIVE ERROR IN RH	RELATIVE ERROR IN T_{mrt}
R^2	0.87	0.77	0.80
CV(RMSE)	4%	6%	10%
NMBE	6%	20%	12%

Table 4 Calculated percentage errors between measured data and the simulation results.

HHHH) significantly reduced the air temperatures by 0.6–2.3°C. The potential reduction in the street-level air temperatures for street canyon B was greater than for canyon A (see Figure 17). The maximum reduction in air temperature occurred at the center and on the left side of the canyon; a smaller reduction was found on the right side due to the effect of shade from buildings. This temperature reduction gradually declined as the height increased. When high-albedo surfaces were used, the mean radiant temperatures in canyon A were higher than for canyon B, due to the increased interreflections of heat from the surrounding surfaces. The maximum mean radiant temperature increased by about 12.1–27.1°C in the shaded area (on the right side), while the changes in the unshaded areas were 7.5°C (see Figure 18).

Figure 19 shows that when only the roads were paved with high-albedo material, the maximum reductions in air temperature in canyons A and B were 1.4°C and 1.9°C, respectively. The use of cool pavements only in parking areas could reduce the air temperature by 0.5–0.7°C, while the use of cool façades gave small temperature reductions of 0.1–0.4°C. Figure 20 shows the increments in mean radiant temperature when high albedo material was used for single surfaces and all surfaces. As expected, the temperatures in the street canyons increased from 12.1°C to 27.1°C for all high-albedo surfaces, which was higher than in the single surface scenarios. When a high-albedo road surface was used, the mean radiant temperature increased by 4.2–24°C. The temperature increments in the blue columns were affected by shade from buildings, and were about 1.5–7 times those in unshaded conditions (orange columns). High ratios of blue to orange columns are found for the single surface scenarios, meaning that the use of low-albedo building façades and parking areas hardly affected the mean radiant temperature.

4.3 AREAS OF EXPOSURE TO RISK OF HEAT STRESS

Hourly average values for the air temperature and relative humidity in street canyons from the ENVI-met simulation were used to assess the level of heat stress risk using Equation (1). Figure 21 presents the diurnal heat stress distribution in street canyons A and B on a day of extreme heat. Based on the average data, the conditions from 9 a.m. to 10 p.m. in most design scenarios were rated at the extreme caution level (32–41°C); the

exceptions were scenarios with low albedo on the road surface, which were rated at the danger level (41–54°C) between 1 p.m. and 3 p.m.

Figure 22 shows the heat stress distributions for the three example cases of C21 (HLHL), C51 (MLML), and C54 (MLLL), in which the road pavement had a low albedo. The danger conditions (shown in red) were found at the center of the street canyons and the area to the left side, as these areas were directly exposed to solar radiation throughout the day. Meanwhile, cooler conditions were found on the right side of the canyons, due to the effect of shade from buildings. The use of high-albedo material in the parking area in C21 could improve the heat stress level on the left side of the canyons.

5. IMPLEMENTATIONS

Figure 23 provides design guidelines of using cool surfaces in regular canyon (A) and avenue canyon (B). The study summarizes the percentages of areas rated at extreme and danger levels in the street canyon when various surface albedos were used. The results show that canyon A had preferable thermal conditions to canyon B. Regarding heat stress mitigation, our results showed that during summer, the use of high-albedo surfaces could not improve the thermal conditions in E-W streets to within the caution level (32–37°C). However, living in canyon A incurs a lower risk of exposure to heat stress than living in canyon B. The left side of the canyon has a long period of exposure to the sun, resulting in some dangerous heat stress conditions, so it should be avoided for outdoor activities.

For achieving maximum reduction of street-level air temperatures during the hottest month, the recommended street canyon type for low-rise residential housing in a hot and humid climate is a deeper street canyon (with a higher H/W). The building shade could protect the road surface from direct exposure to solar radiation, resulting in lower air temperature. Additionally, it also lessens the mean radiant temperature emitted from low-albedo road pavements. For the avenue canyon (H/W = 0.6), the recommended design primarily uses medium to high albedo materials for all surface pavements. This design could provide 97–100% of the areas within extreme conditions.
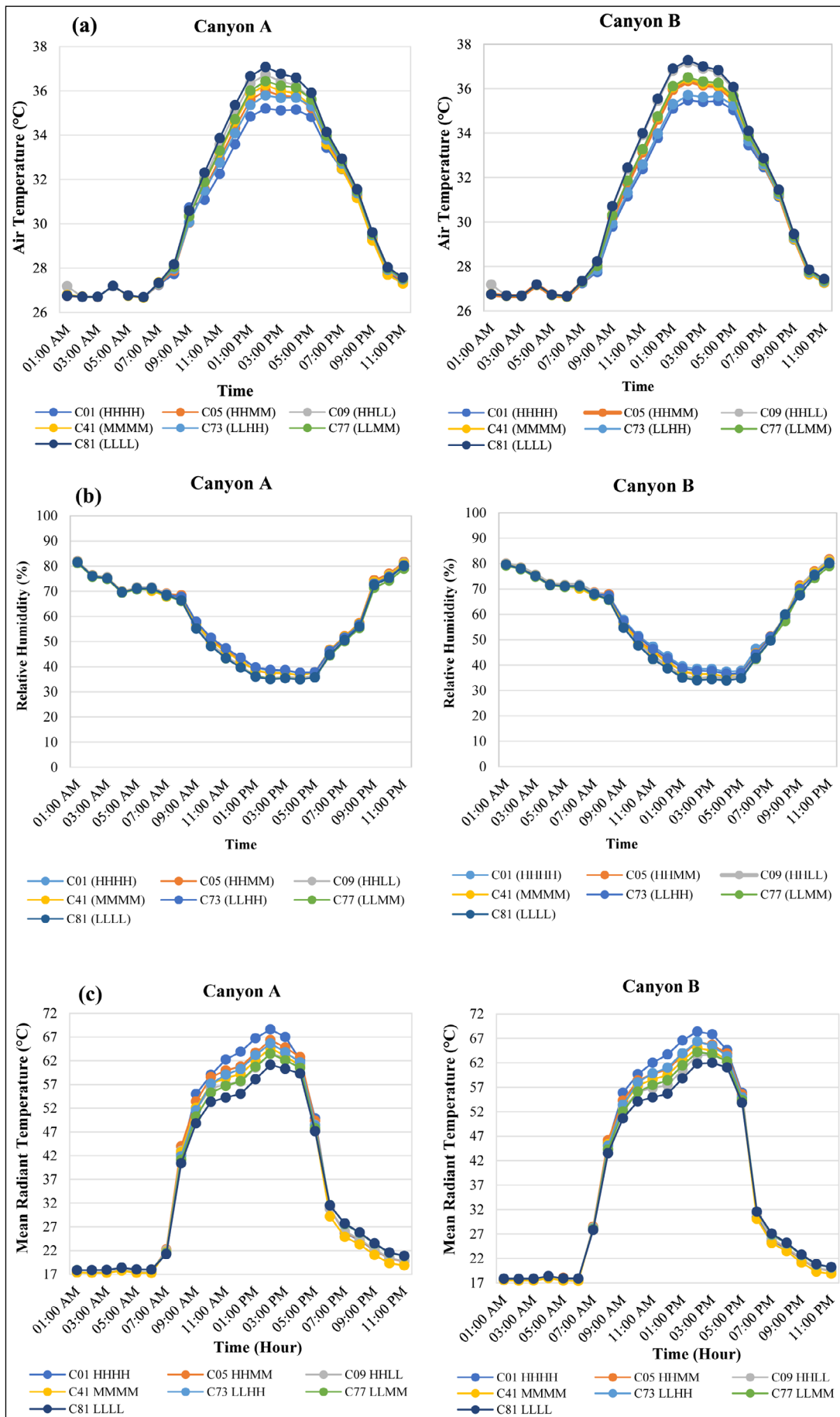
Figure 9 Hourly average values of **(a)** air temperature, **(b)** relative humidity, and **(c)** mean radiant temperature for street canyons A and B. The 4-letter code (XXXX) after each design scenario represents the albedo value applied to the upper façade, lower façade, parking area, and road, respectively, when H, M, and L is high, medium, and low albedo values.
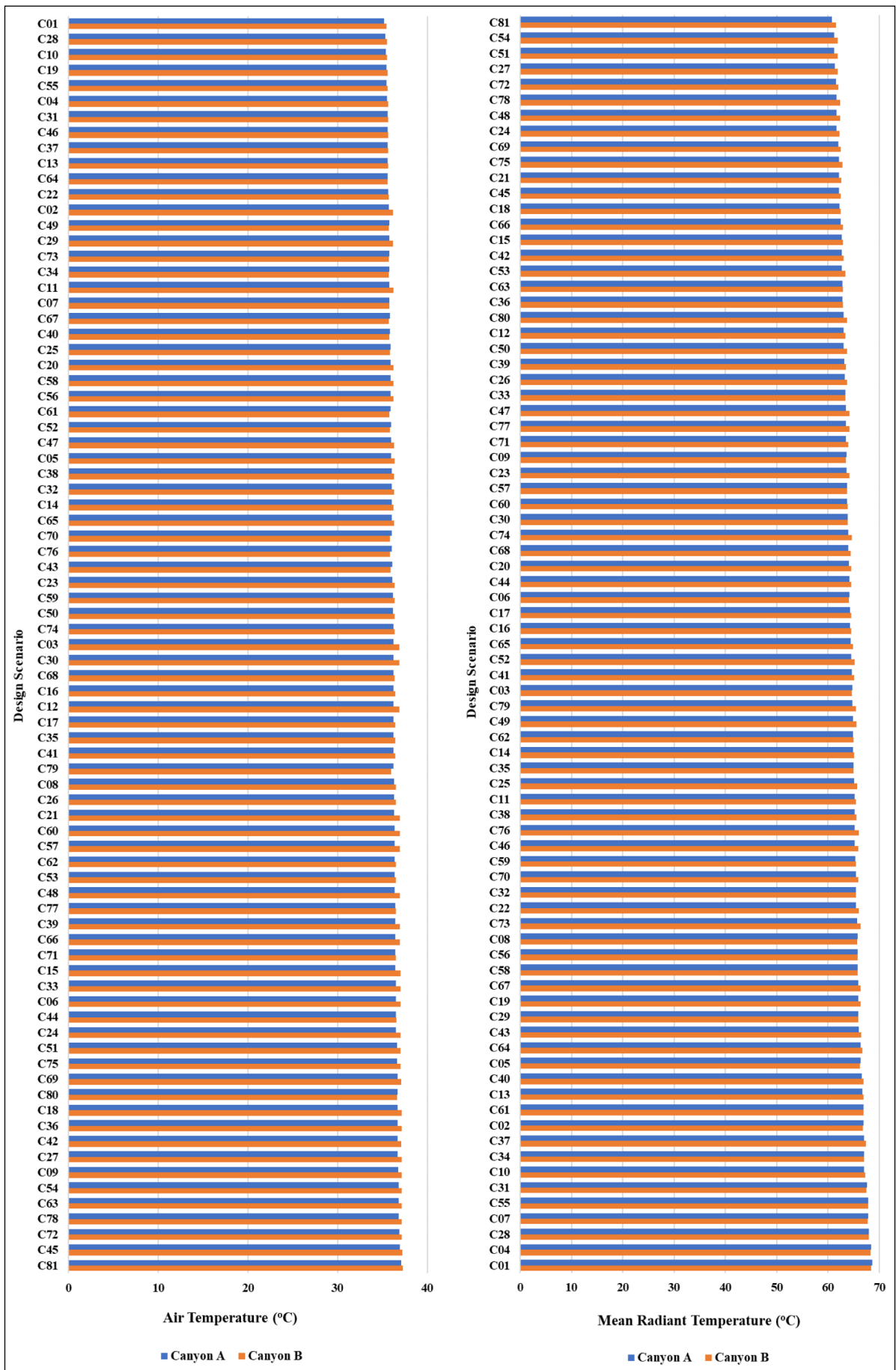
Figure 10 Rankings of average air temperatures (left) and mean radiant temperatures (right) at 2 p.m. for 81 design scenarios for canyons A and B.
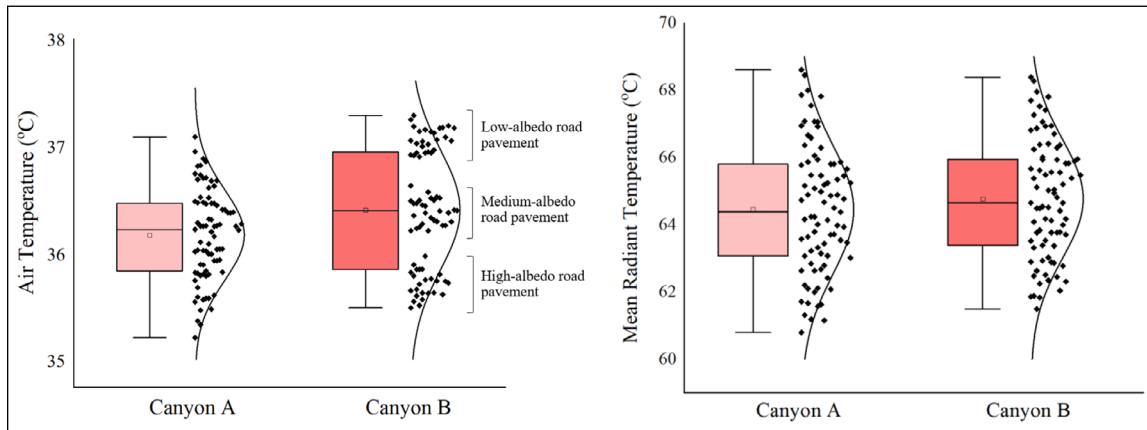
Figure 11 Distributions of average air temperatures (left) and mean radiant temperatures (right) at 2 p.m. for 81 design scenarios.
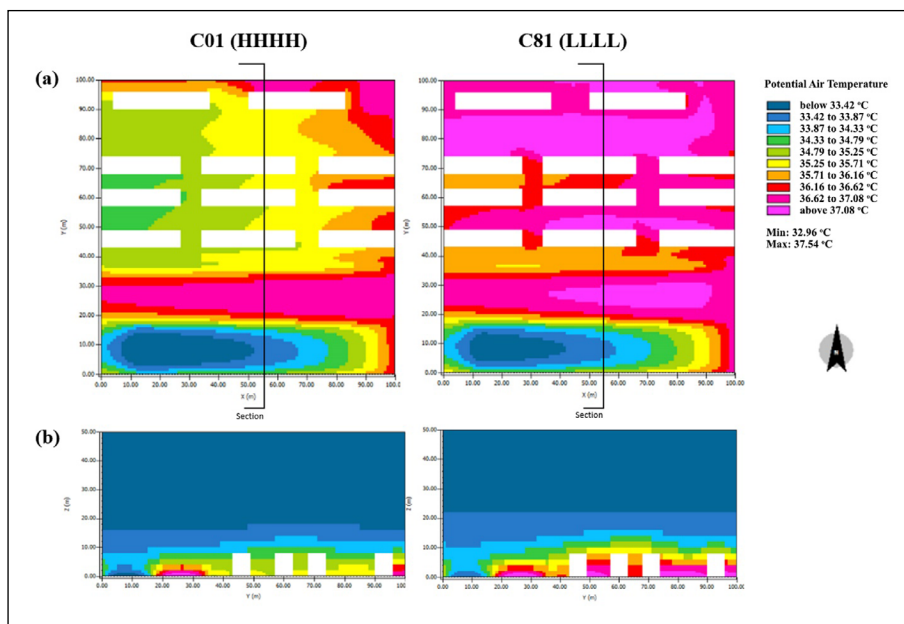

Figure 12 (a) Results of the ENVI-met simulation of air temperature for cases 01 and 81, and **(b)** sections.
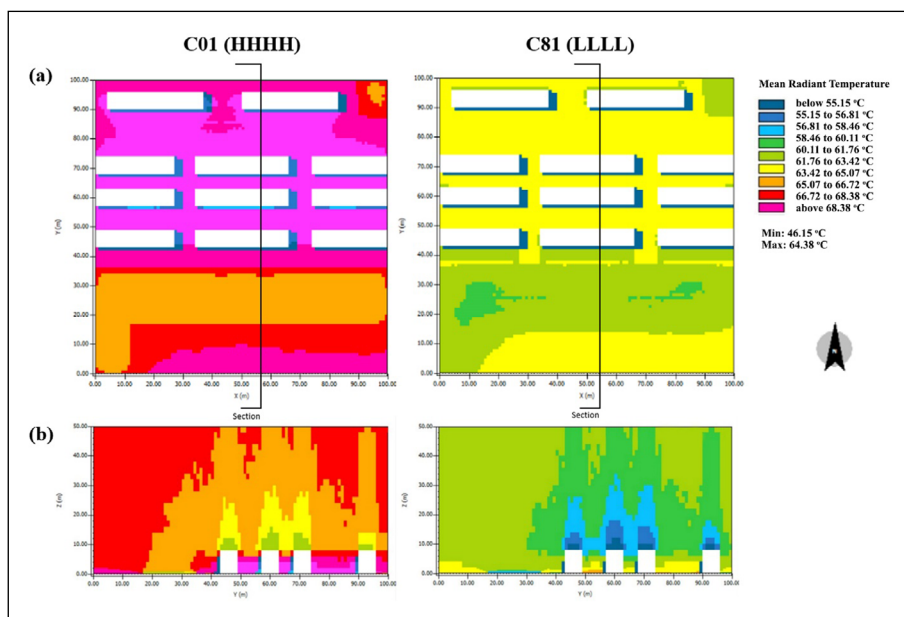

Figure 13 (a) Results of the ENVI-met simulation of mean radiant temperature for cases 01 and 81, and **(b)** sections.
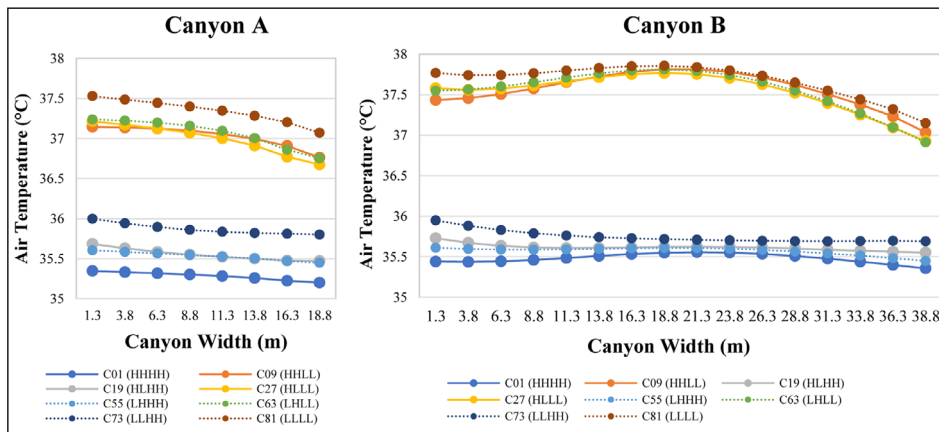
Figure 14 Average air temperatures across canyons A (left) and B (right) at a height of 1.4 m.
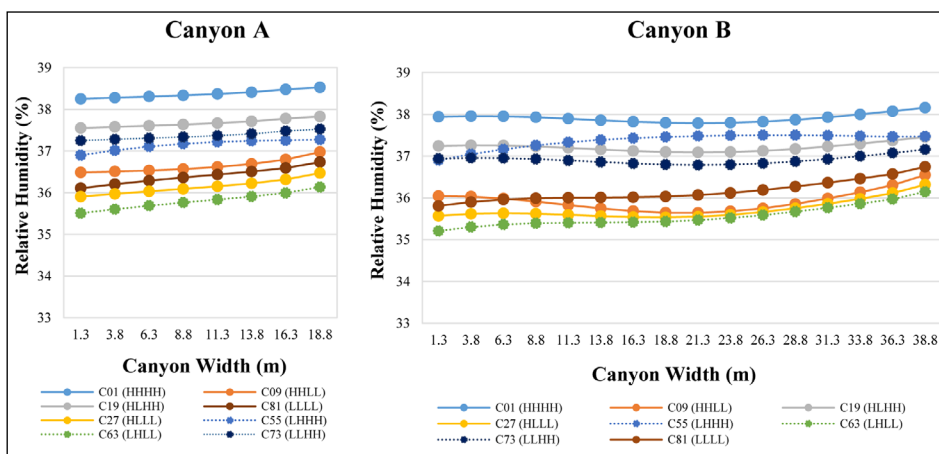

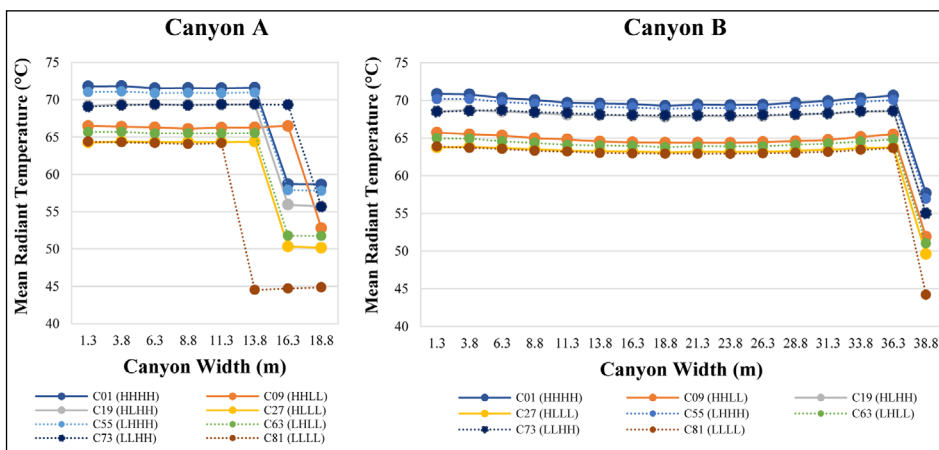**Figure 15** Average relative humidity across canyons A (left) and B (right) at a height of 1.4 m.

Figure 16 Average mean radiant temperatures across canyons A (left) and B (right) at a height of 1.4 m.

6. DISCUSSION

Due to issues related to global warming, the problem of heat-related deaths arising from increases in urban temperature has become a significant concern in terms of outdoor activities. Improving the thermal conditions for pedestrians in E-W street canyons poses a challenge, as there is little shade from buildings, especially in street canyons with low H/W ratios (Srivanit & Jareemit 2020;

Zhang et al. 2021; Takebayashi & Moriyama 2012a). In this study, we investigated several combinations of paving and wall surfaces with various surface albedos to find the potential reductions in air temperature and heat stress mitigation in street canyons with limited surrounding shade under extreme conditions.

The use of high-albedo materials for different regular and avenue street canyon surfaces showed different effects. To better understand these effects, a Pearson
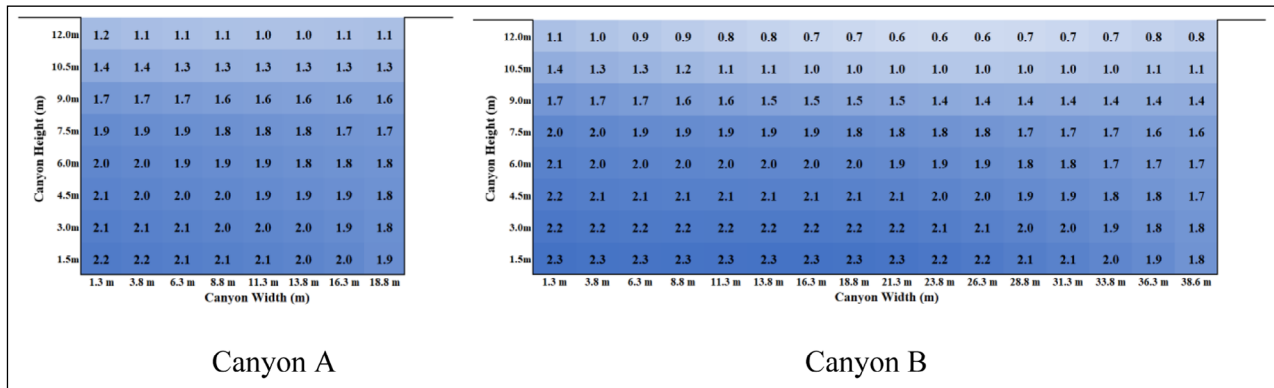
Figure 17 Maximum reductions in air temperature over the cross-sections of street canyons A and B: comparison of cases C81 and C01.
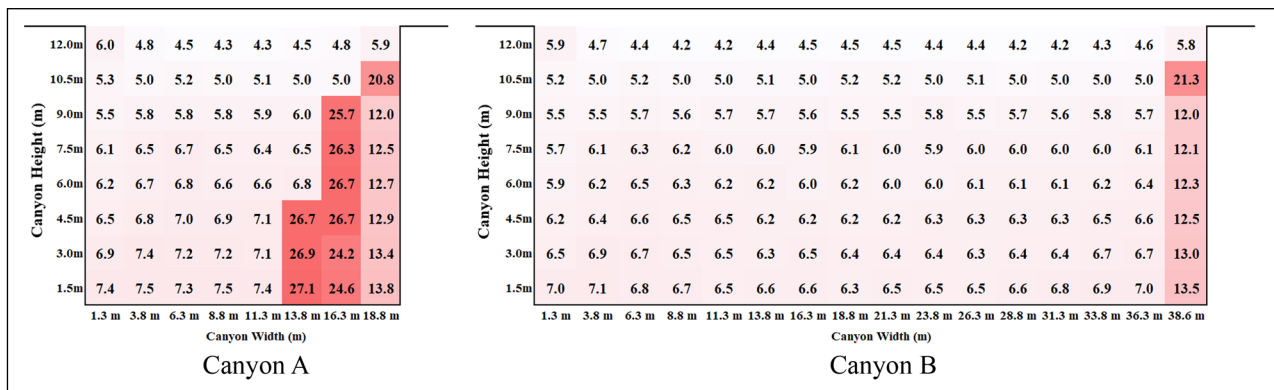

Figure 18 Maximum increments in mean radiant temperature over the cross-sections of street canyons A and B: comparison of cases C81 and C01.
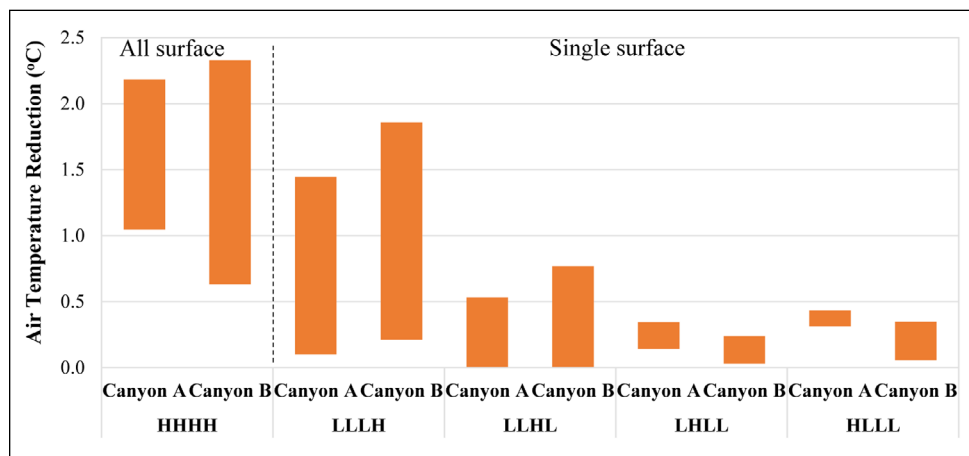

Figure 19 Reductions in air temperature of street canyons when high-albedo material was used for single surfaces and all surfaces, compared to the base case (C81, LLLL).

correlation analysis was used to assess the impact of surface albedo on thermal conditions. Pairs of variables with a high statistical significance between them are highlighted in gray in Table 5. A regression analysis (enter method) was performed to identify significant design factors that influenced the thermal conditions of street canyons A and B based on the standardized coefficient (Beta), as shown in Table 6. From this analysis, we observed that the road surface was significantly correlated with both air temperature and mean radiant temperature for canyons A and B, which aligns with the

findings of Yang and Li (2015). In both street canyons, the road pavement had the highest impact on changes in air temperature and mean radiant temperature. In the case of canyon A, the surface of the parking area had a secondary impact on air temperature, although this effect was not observed in canyon B. The road surface and lower façade had a significant negative effect on the mean radiant temperature in both canyons A and B (Salata et al. 2015; Taleghani & Berardi 2018; Salvati et al. 2022). There was no significant correlation with the upper façade, meaning that increasing the albedo
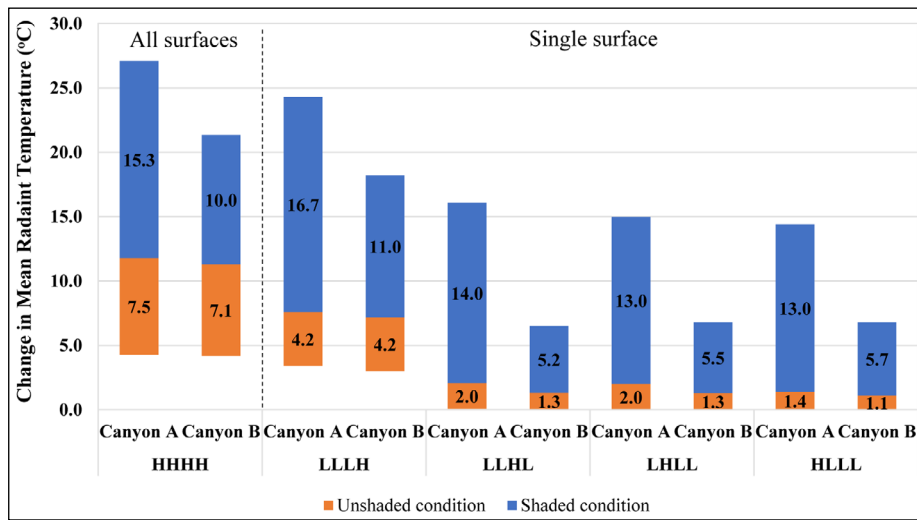
Figure 20 Increase in mean radiant temperature in street canyons when high-albedo material was used for single surfaces and all surfaces, compared to the base case (C81, LLLL) (the blue columns show the temperature increments that occurred in the shaded areas on the right side of each street canyon).
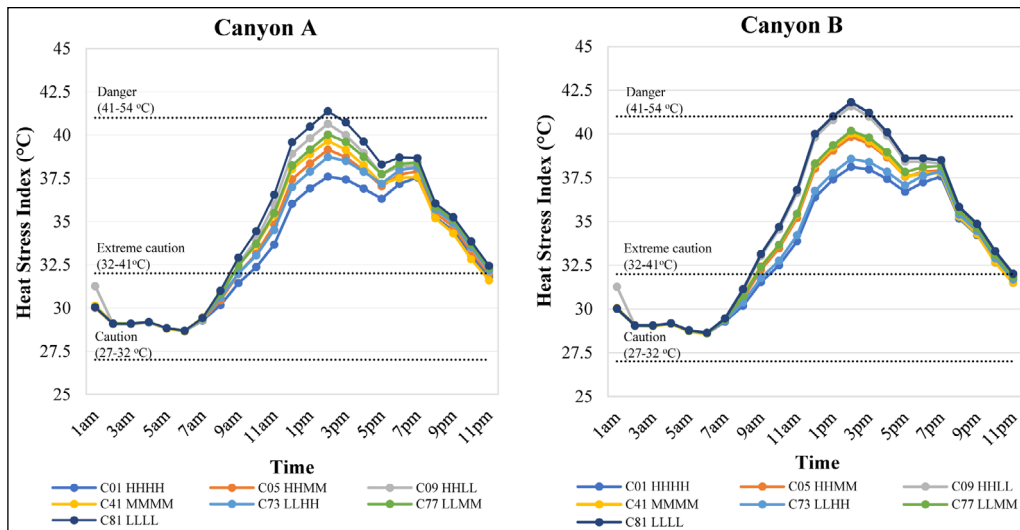

Figure 21 Calculated hourly average values for heat stress level in canyons A and B, for seven example scenarios.

of the upper façade did not lead to changes in the air temperature or mean radiant temperature at the street level.

The regression analysis was able to explain how the rankings of air temperatures in canyon A showed different patterns from those of canyon B (Figure 24). However, in some scenarios, the average air temperatures in canyon A were lower than in canyon B. Based on the results, the scenarios could be classified into three types:

Group 1: The average air temperatures in canyon B were about 0.01–0.3°C lower than in canyon A. In these design scenarios, the road was paved with a high-albedo surface, while the parking areas had a low to medium albedo.

Group 2: The average air temperatures in canyon B were 0.25°C higher than in canyon A. In these

scenarios, the road and parking surfaces were paved with high-albedo materials.

Group 3: The average air temperatures in canyon B were 0.25–0.69°C higher than in canyon A. In these scenarios, materials with low albedos were used for the road surfaces.

The regression analysis showed that the albedo of the road surface and the width of the street canyon significantly affected the street-level air temperatures. The use of a high-albedo material over a large surface means that more solar radiation can be reflected into the surrounding air (Qin 2015; Erell et al. 2014; Salvati et al. 2022). Qin (2015) reported that increasing the surface albedo in a canyon with H/W ≤ 1 could effectively increase the ability to reflect solar radiation to the sky. However, in our study showed contrast that the air temperature reduction in canyon B (H/W = 0.6) was higher than in
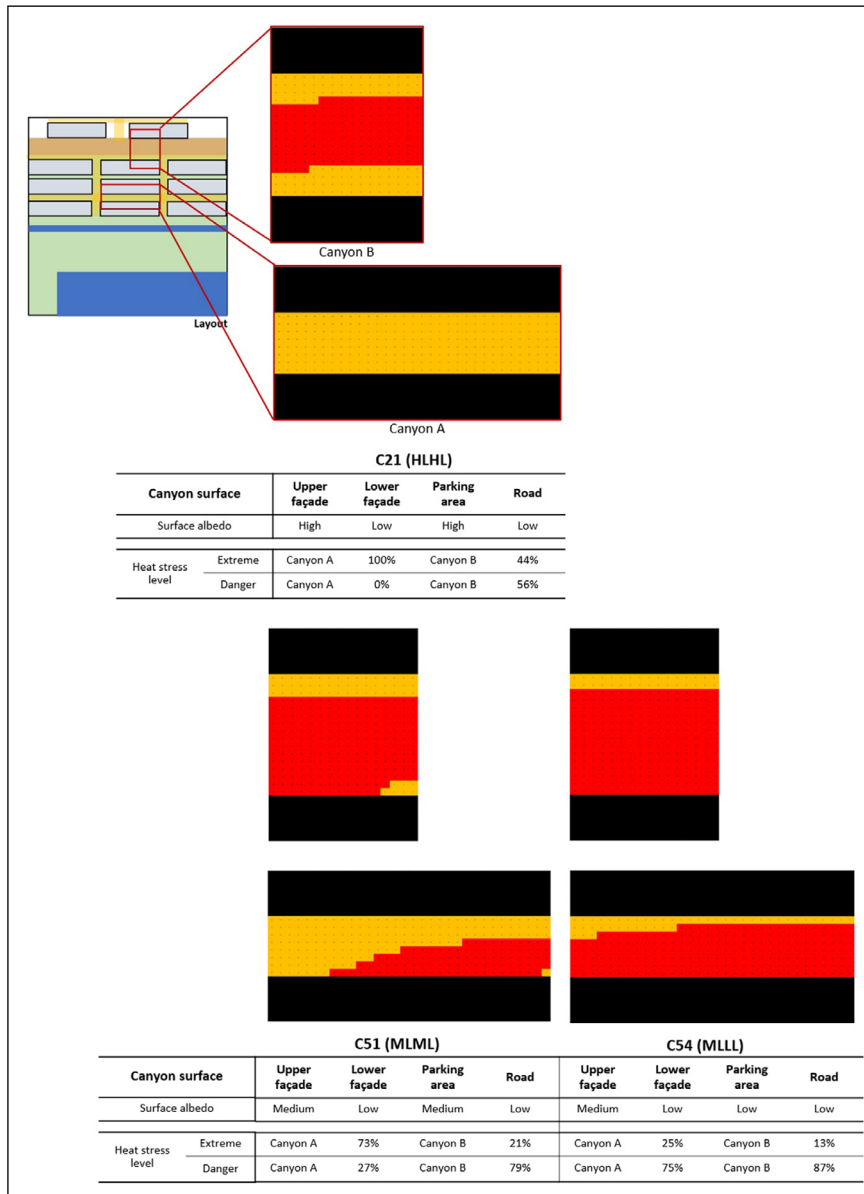
C21 (HLHL)

Canyon surface	Upper façade	Lower façade	Parking area	Road
Surface albedo	High	Low	High	Low

Heat stress level		Upper façade	Lower façade	Parking area	Road
	Extreme	Canyon A	100%	Canyon B	44%
	Danger	Canyon A	0%	Canyon B	56%

	C51 (MLML)				**C54 (MLLL)**			
Canyon surface	Upper façade	Lower façade	Parking area	Road	Upper façade	Lower façade	Parking area	Road
Surface albedo	Medium	Low	Medium	Low	Medium	Low	Low	Low

Heat stress level		Upper façade	Lower façade	Parking area	Road	Upper façade	Lower façade	Parking area	Road
	Extreme	Canyon A	73%	Canyon B	21%	Canyon A	25%	Canyon B	13%
	Danger	Canyon A	27%	Canyon B	79%	Canyon A	75%	Canyon B	87%

Figure 22 Areas of the street canyons that were rated at extreme and dangerous levels in the three example scenarios.

Surface pavement albedo		Design	Extreme condition area (32°C–41°C)	Danger condition area (41°C–54°C)
Road	Parking area			
L	L or M	Canyon A	0%–75%	25%–100%
		Canyon B	0%–18%	82%–100%
L M	H L or M	Canyon A	64%–78%	22%–36%
L	M or H	Canyon B	21%–50%	50%–79%
M or H	L, M, or H	Canyon A	**100%**	**0%**
		Canyon B	**97%–100%**	**0%–3%**

Figure 23 Canyon albedo characteristics, classified based on the percentage of the area rated at extreme or dangerous levels.

Note: Wall materials may have low, medium, or high surface albedos.

PEARSON CORRELATION		UPPER FAÇADE	LOWER FAÇADE	PARKING	ROAD	T_{air} CANYON A	T_{mrt} CANYON A	T_{air} CANYON B	T_{mrt} CANYON B
Upper façade	Pearson	1							
	Sig. (2-tailed)								
	N	81							
Lower façade	Pearson	.000	1						
	Sig. (2-tailed)	1.000							
	N	81	81						
Parking	Pearson	.000	.000	1					
	Sig. (2-tailed)	1.000	1.000						
	N	81	81	81					
Road	Pearson	.000	.000	.000	1				
	Sig. (2-tailed)	1.000	1.000	1.000					
	N	81	81	81	81				
T_{air} **Canyon A**	Pearson	−.215	−.183	−**.459****	−**.811****	1			
	Sig. (2-tailed)	.054	.102	.000	.000				
	N	81	81	81	81	81			
T_{mrt} **Canyon A**	Pearson	.126	**.490****	.208	**.805****	−**.884****	1		
	Sig. (2-tailed)	.262	.000	.062	.000	.000			
	N	81	81	81	81	81	81		
T_{air} **Canyon B**	Pearson	−.050	−.047	−.194	−**.953****	**.924****	−**.872****	1	
	Sig. (2-tailed)	.656	.678	.083	.000	.000	.000		
	N	81	81	81	81	81	81	81	
T_{mrt} **Canyon B**	Pearson	.095	**.375****	.221	**.862****	−**.909****	**.991****	−**.924****	1
	Sig. (2-tailed)	.400	.001	.048	.000	.000	.000	.000	
	N	81	81	81	81	81	81	81	81

Table 5 Results of a Pearson correlation analysis of the surface albedos and thermal conditions of two street canyons.

**. Correlation is significant at the 0.01 level (2-tailed).

(-) A minus sign represents a negative effect.

PARAMETERS	MODEL	UNSTANDARDIZED COEFFICIENTS		STANDARDIZED COEFFICIENTS	T	SIG.	95.0% CONFIDENCE INTERVAL FOR B	
		B	STD. ERROR	BETA			BOTTOM BOUND	UPPER BOUND
T_{air} Canyon A	(Constant)	37.543	.065		573.230	.000	37.412	37.673
	Road	−1.655	.084	−.811	−19.758	.000	−1.822	−1.489
	Parking	−.936	.084	−.459	−11.175	.000	−1.103	−.769
T_{air} Canyon B	(Constant)	37.766	.052		721.479	.000	37.662	37.871
	Road	−2.571	.092	−.953	−28.068	.000	−2.753	−2.388
T_{mrt} Canyon A	(Constant)	58.967	.233		253.203	.000	58.503	59.431
	Road	7.428	.351	.805	21.140	.000	6.729	8.128
	Lower façade	3.792	.295	.490	12.864	.000	3.205	4.379
T_{mrt} Canyon B	(Constant)	58.773	.216		272.477	.000	58.343	59.202
	Road	7.348	.254	.862	28.979	.000	6.843	7.853
	Lower façade	2.686	.213	.375	12.629	.000	2.263	3.110

Table 6 Results of a regression analysis of the surface albedos and thermal conditions of two street canyons.

canyon A (H/W = 1.2), since canyon B had a larger area of road pavement and fewer shaded areas than canyon A.

A large difference in air temperature between canyons B and A was seen in Group 3, where the road had a low albedo. For Group 1, the use of a low-albedo material in the parking area raised the air temperature near the wall (see Figure 25), causing the air temperatures in canyon A to be slightly higher than in canyon B. This was because canyon A had buildings that were relatively close together, with increased heat reflection from the canyon surfaces, while the inter-reflection effect between vertical surfaces in the avenue canyon (canyon B) was small (Salvati et al. 2022; Zhang et al. 2022; Yang & Li 2015).

Considering the effect of road pavement on thermal conditions in regular and avenue street canyons. Figure 26 presents the correlation plots of the air temperatures and mean radiant temperatures in canyon A compared to canyon B. It was found that the air temperatures and mean radiant temperatures in canyon A and B were fairly similar when applied to high-albedo road pavement. However, the temperature differences became larger when the road was paved with low albedo material. Air temperature and mean radiant temperatures in canyon B were about 4% higher than in canyon A. It was because some parts of the surface areas in canyon A were shaded by nearby buildings, which lesson heat stored in that low albedo pavement.

A few researchers (Salvati et al. 2022; Zhang et al. 2022) have investigated the effect of wall materials in terms of improving thermal conditions in street canyons.
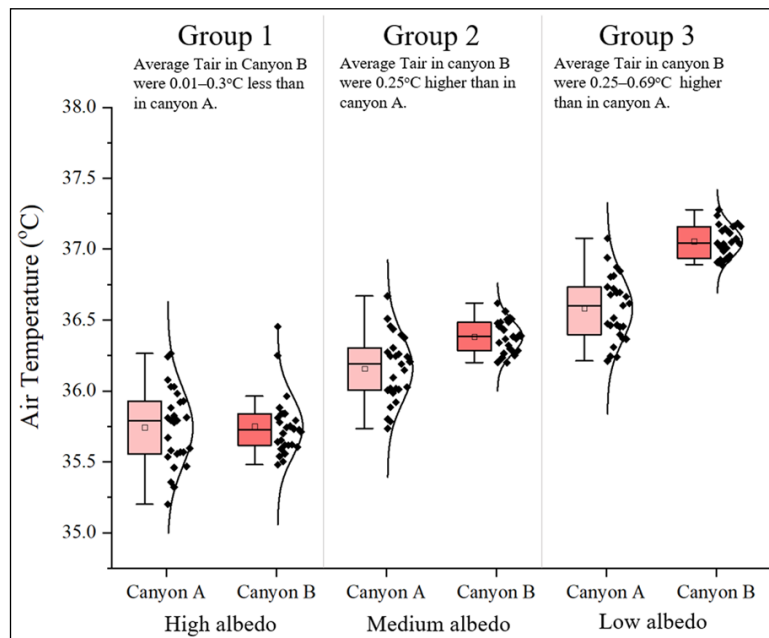

Figure 24 Classification of air temperature distributions in canyons A and B when applied with different road surface albedos.
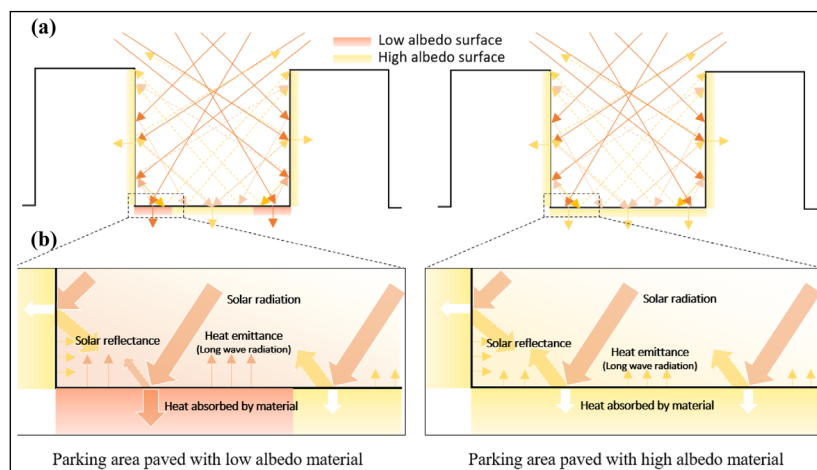

Figure 25 (a) Heat interreflections in street canyon when the parking area was paved with low and high albedo materials. **(b)** Enlarge zoom regions of solar heat reflectance and trapping effects near building façade.
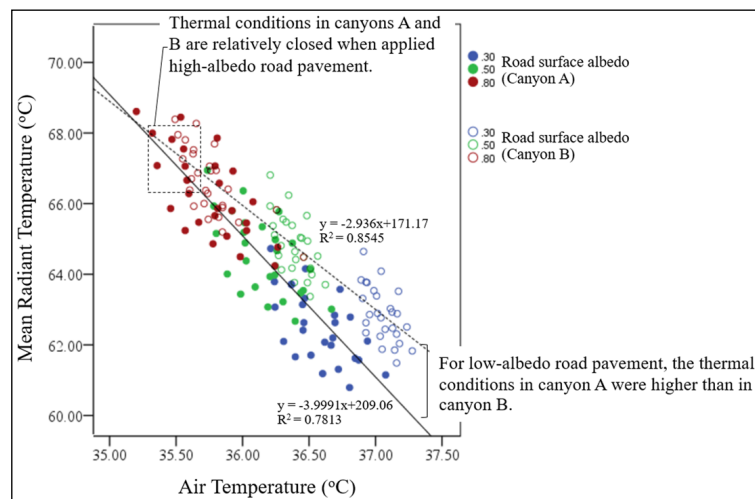
Figure 26 Relationship between air temperatures and mean radiant temperatures in canyons A (shown in blue) and B (shown in orange).

They found that the use of a high reflectivity material for the lower façade in street canyon with H/W = 0.75 did not significantly affect the street-level air temperatures, but worsened the outdoor thermal comfort conditions due to a rise in mean radiant temperature. This study showed that the use of cool façades significantly raises the mean radiant temperature near the wall. However, they do not impact the air temperature in street canyons, due to the high solar angle. Consequently, a cool façade receives less solar radiation, leading to a lower impact on the air temperature (Kotopouleas et al. 2021).

At the pedestrian level, cool surfaces provided significant reductions in air temperature in unshaded areas. In this study, the highest air temperature reduction found in unshaded areas was 2.3°C, while that in shaded areas was 1.8°C. This was because shade from buildings prevented the road surface from being directly exposed to solar radiation, which reduced the surface temperature. This effect significantly lowered the sensible heat flux emitted from the low-albedo surfaces to the surrounding air (Rahman et al. 2021).

For mitigation of heat stress for E-W oriented streets at peak time (2 p.m.), a medium- to high-albedo material should be used for the road surface. This could reduce the risk of exposure to a dangerous level of heat stress (41–54°C) by 98–100%. Heat mitigation strategies in other designs with low albedo pavements in areas with limited tree planting have been based on the use of other cooling techniques. For example, previous studies (Jareemit & Srivanit 2022; Garcia-Nevado et al. 2020) have suggested the use of an overhead shading structure to protect the area directly exposed to solar radiation at the center and to the left of the canyon.

For the study's limitations, the thermal conditions and heat stress levels were assessed under the worst conditions in summer, along an E-W-oriented street with low-rise buildings. During the summer season, when

the sun's path lies in the northern hemisphere, there is a minimal advantage in terms of cooling from building shade on the right side of the street canyon. For a more comprehensive understanding of the advantages and limitations of cool pavements, future studies should conduct analyses of streets with varying orientations and building heights. Exploring the extent of heat mitigation in different seasons would also be beneficial.

In this study, we used the HI to assess the hotspot areas in two street canyons and the risk levels of outdoor activities. These calculations were based on air temperature and relative humidity. It was interesting to note that the heat stress level increased as the air temperature rose. Researchers have suggested that cool pavements could help to lower the air temperature and the heat stress levels; however, cool pavements reflect more solar heat to the surrounding air, causing a high mean radiant temperature that significantly reduces thermal comfort. This study did not investigate the impact of cool pavements on outdoor thermal comfort, and it will be important to consider heat stress mitigation and outdoor thermal comfort in future work.

We note that the street canyon was modeled without parking areas or trees; however, in an actual environment, these elements are important, as they can cause an increase in heat reflections, ultimately affecting the thermal conditions in the street canyon.

7. CONCLUSION

This paper has assessed the combined effect of façade and paving surface albedos on the thermal conditions and heat stress levels in a low-rise housing project in Bangkok, Thailand. The distributions of air temperature, relative humidity, and mean radiant temperature across two different street canyons in extreme conditions were calculated using the ENVI-met model. The simulation results were validated based on the field data with

acceptable errors (R^2 = 0.8, CV(RMSE) = 10%, and NMBE = 12%). The simulated air temperature and relative humidity at peak hours were used to calculate the heat stress level for each design scenario.

The main findings were as follows:

1) An effective strategy for reducing the extreme heat accumulated in street canyons is recommended based on the use of medium to high albedos for road and parking pavements. The study revealed that when high-albedo road pavement was used, the air temperatures and mean radiant temperatures in both canyons A and B showed considerable similarity. The maximum reductions in temperature of street canyons with H/W = 1.2 and H/W = 0.6 were 2.1°C and 2.3°C, respectively. However, the use of cool pavements inversely increased the mean radiant temperatures, especially for the deeper street canyon. The effect of multiple heat reflections from the surrounding surfaces caused the maximum increment in mean radiant temperature in canyon A to be 3.5°C higher than in canyon B.

2) Regarding the influence of surface albedo on street-level thermal conditions, we found that a reflective road pavement was a significant contributor to the air and mean radiant temperatures in street canyons due to its large area. The use of cool façade did not affect the street-level air temperatures, but had a secondary influence on the increase in mean radiant temperature.

3) Shade from buildings positively impacted the reductions in mean radiant temperature in the canyons with low-albedo road pavements. Shading can reduce the floor temperature, thus decreasing the amount of long-wave radiation emitted to the surroundings.

4) During hot summer days, a scenario with cool pavements gave a reduction in extreme heat conditions at 2 p.m., when all areas in the E-W-oriented street canyon had a heat stress index ranging from 32–41°C. The deeper canyon provided better thermal conditions for outdoor activities than the avenue canyon. Furthermore, during summer afternoons (1 p.m. to 3 p.m.), activities should carry out on the right side of the canyon, shaded by a nearby building.

Our findings illustrate how single and combined surface albedos could improve thermal conditions in two types of street canyons in a low-rise affordable housing project in Thailand. The benefits and limitations on the use of cool façades and pavements were explored. Architects and urban planners can use our preliminary guidelines in their landscape designs to improve outdoor environments and reduce exposure to dangerous heat stress conditions.

COMPETING INTERESTS

The authors have no competing interests to declare.

AUTHOR AFFILIATIONS

Wacharakorn Maneechote
Faculty of Architecture and Planning, Thammasat University, Pathumthani 12121, Thailand

Jiying Liu orcid.org/0000-0001-7385-6959
School of Thermal Engineering, Shandong Jianzhu University, Jinan 250101, China

Daranee Jareemit orcid.org/0000-0001-9312-0367
Faculty of Architecture and Planning, Thammasat University, Pathumthani 12121, Thailand; Thammasat University Research Unit in Architecture for Sustainable Living and Environment, Thammasat University, Pathumthani 12121, Thailand

REFERENCES

Acharya, T, Riehl, B and **Fuchs, A.** 2021. Effects of albedo and thermal inertia on pavement surface temperatures with convective boundary conditions—A CFD Study. *Processes,* 9(11): Article 11. DOI: https://doi.org/10.3390/pr9112078

Afiq, WM, Azwadi, CSN and **Saqr, KM.** 2012. Effects of buildings aspect ratio, wind speed and wind direction on flow structure and pollutant dispersion in symmetric street canyons: A review. *International Journal of Mechanical and Materials Engineering,* 7(2): 158–165. Available online: https://www.semanticscholar.org/paper/Effects-of-buildings-aspect-ratio%2C-wind-speed-and-a-Afiq-Azwadi/e86753493e5eb8fc6275a094a3202acdbed38877.

Anand, J and **Sailor, DJ.** 2022. Role of pavement radiative and thermal properties in reducing excess heat in cities. *Solar Energy,* 242: 413–423. DOI: https://doi.org/10.1016/j.solener.2021.10.056

Arifwidodo, SD and **Chandrasiri, O.** 2020. Urban heat stress and human health in Bangkok, Thailand. *Environmental Research,* 185: 109398. DOI: https://doi.org/10.1016/j.envres.2020.109398

Bruse, M. 2004. ENVI-met 3.0: Updated model overview.

Bruse, M and **Fleer, H.** 1998. Simulating surface–plant–air interactions inside urban environments with a three dimensional numerical model. *Environmental Modelling & Software,* 13(3): 373–384. DOI: https://doi.org/10.1016/S1364-8152(98)00042-5

Choi, Y, Lee, S and **Moon, H.** 2018. Urban physical environments and the duration of high air temperature:

Focusing on solar radiation trapping effects. *Sustainability,* 10(12): Article 12. DOI: https://doi.org/10.3390/su10124837

Crank, PJ, Middel, A, Wagner, M, Hoots, D, Smith, M and **Brazel, A.** 2020. Validation of seasonal mean radiant temperature simulations in hot arid urban climates. *Science of the Total Environment,* 749: 141392. DOI: https://doi.org/10.1016/j.scitotenv.2020.141392

Department of Disease Control, Ministry of Public Health. 2022. Heat stroke is a risk of severe symptoms and death [Government Website]. Department of Disease Control [online access at https://ddc.moph.go.th/odpc7/news.php?news=24196&deptcode=odpc7].

Erell, E, Pearlmutter, D, Boneh, D and **Kutiel, PB.** 2014. Effect of high-albedo materials on pedestrian heat stress in urban street canyons. *Urban Climate,* 10: 367–386. DOI: https://doi.org/10.1016/j.uclim.2013.10.005

Falasca, S, Ciancio, V, Salata, F, Golasi, I, Rosso, F and **Curci, G.** 2019. High albedo materials to counteract heat waves in cities: An assessment of meteorology, buildings energy needs and pedestrian thermal comfort. *Building and Environment,* 163: 106242. DOI: https://doi.org/10.1016/j.buildenv.2019.106242

Fang, Z, He, H, Guo, Z, Zheng, Z and **Feng, X.** 2023. Daily variation of ground radiation in unshaded and shaded environments and the effect on mean radiant temperature. *Case Studies in Thermal Engineering,* 43: 102791. DOI: https://doi.org/10.1016/j.csite.2023.102791

Ford, L and **Ford, LR.** 2000. The spaces between buildings. JHU Press. DOI: https://doi.org/10.56021/9780801863301

Garcia-Nevado, E, Beckers, B and **Coch, H.** 2020. Assessing the cooling effect of urban textile shading devices through time-lapse thermography. *Sustainable Cities and Society,* 63: 102458. DOI: https://doi.org/10.1016/j.scs.2020.102458

Greater London Authority. 2006. London urban heat island (LUHI): A summary for decision makers. ISO 7726:1998 Available online: https://www.iso.org/cms/render/live/en/sites/isoorg/contents/data/standard/01/45/14562.html (accessed on 18 November 2021).

Jareemit, D and **Canyookt, P.** 2020. Residential cluster design and potential improvement for maximum energy performance and outdoor thermal comfort on a hot summer in Thailand. *International Journal of Low-Carbon Technologies*, ctaa091. DOI: https://doi.org/10.1093/ijlct/ctaa091

Jareemit, D and **Srivanit, M.** 2022. A comparative study of cooling performance and thermal comfort under street market shades and tree canopies in tropical savanna climate. *Sustainability,* 14(8): Article 8. DOI: https://doi.org/10.3390/su14084653

Kachenchart, B, Kamlangkla, C, Puttanapong, N and **Limsakul, A.** 2021. Urbanization effects on surface air temperature trends in Thailand during 1970–2019. *Environmental Engineering Research,* 26(5). DOI: https://doi.org/10.4491/eer.2020.378

Kotopouleas, A, Giridharan, R, Nikolopoulou, M, Watkins, R and **Yeninarcilar, M.** 2021. Experimental investigation of the impact of urban fabric on canyon albedo using a 1:10 scaled physical model. *Solar Energy,* 230: 449–461. DOI: https://doi.org/10.1016/j.solener.2021.09.074

Leetongin, P, Inprom, N, Srivanit, M and **Jareemit, D.** 2022. The Effects of Design Combinations of Surface Materials and Plants on Outdoor Thermal Conditions during Summer around a Single-Detached House: A Numerical Analysis. *Nakhara: Journal of Environmental Design and Planning,* 21(3): Article 3. DOI: https://doi.org/10.54028/NJ202221218

Lopez-Cabeza, VP, Alzate-Gaviria, S, Diz-Mellado, E, Rivera-Gomez, C and **Galan-Marin, C.** 2022. Albedo influence on the microclimate and thermal comfort of courtyards under Mediterranean hot summer climate conditions. *Sustainable Cities and Society,* 81: 103872. DOI: https://doi.org/10.1016/j.scs.2022.103872

Maggiotto, G, Buccolieri, R, Santo, MA, Sabatino, SD and **Leo, LS.** 2014. Study of the urban heat island in Lecce (Italy) by means of ADMS and ENVI-MET. *International Journal of Environment and Pollution,* 55(1–4): 41. DOI: https://doi.org/10.1504/IJEP.2014.065903

Marks, D and **Connell, J.** 2023. Unequal and unjust: The political ecology of Bangkok's increasing urban heat island. *Urban Studies*, 00420980221140999. DOI: https://doi.org/10.1177/00420980221140999

Mohammad, P, Aghlmand, S, Fadaei, A, Gachkar, S, Gachkar, D and **Karimi, A.** 2021. Evaluating the role of the albedo of material and vegetation scenarios along the urban street canyon for improving pedestrian thermal comfort outdoors. *Urban Climate,* 40: 100993. DOI: https://doi.org/10.1016/j.uclim.2021.100993

Nasrollahi, N, Ghosouri, A, Khodakarami, J and **Taleghani, M.** 2020. Heat-mitigation strategies to improve pedestrian thermal comfort in urban environments: A review. *Sustainability,* 12(23): Article 23. DOI: https://doi.org/10.3390/su122310000

National Weather Service 2023 NWS Experimental HeatRisk. National Ocean and Atmospheric Administration [online access at chrome-extension://efaidnbmnnnibpcajpcglclefindmkaj/https://www.wrh.noaa.gov/wrh/heatrisk/pdf/HeatRisk_More_Info_Web.pdf].

Nazarian, N, Dumas, N, Kleissl, J and **Norford, L.** 2019. Effectiveness of cool walls on cooling load and urban temperature in a tropical climate. *Energy and Buildings,* 187: 144–162. DOI: https://doi.org/10.1016/j.enbuild.2019.01.022

Oke, TR, Mills, G, Christen, A and **Voogt, JA.** 2017. Urban climates. Cambridge University Press. DOI: https://doi.org/10.1017/9781139016476

Parsaee, M, Joybari, MM, Mirzaei, PA and **Haghighat, F.** 2019. Urban heat island, urban climate maps and urban development policies and action plans. *Environmental Technology & Innovation,* 14: 100341. DOI: https://doi.org/10.1016/j.eti.2019.100341

Probst, N, Bach, P, Cook, L, Maurer, M and **Leitão, J.** 2022. Blue green systems for urban heat mitigation: Mechanisms, effectiveness and research directions. *Blue-Green Systems,* 4. DOI: https://doi.org/10.2166/bgs.2022.028

Qin, Y. 2015. Urban canyon albedo and its implication on the use of reflective cool pavements. *Energy and Buildings,* 96: 86–94. DOI: https://doi.org/10.1016/j.enbuild.2015.03.005

Rahman, MA, Dervishi, V, Moser-Reischl, A, Ludwig, F, Pretzsch, H, Rötzer, T and **Pauleit, S.** 2021. Comparative analysis of shade and underlying surfaces on cooling effect. *Urban Forestry & Urban Greening,* 63: 127223. DOI: https://doi.org/10.1016/j.ufug.2021.127223

Rothfusz, LP. 1990. The heat index "equation" (or, more than you ever wanted to know about heat index) [Tech. Attachment, SR/SSD 90–23]. [online access at http://www.srh.noaa.gov/images/ffc/pdf/ta_htindx.PDF].

Ruiz, GR and **Bandera, CF.** 2017. Validation of calibrated energy models: common errors. *Energies,* 10(10): Article 10. DOI: https://doi.org/10.3390/en10101587

Salvati, A, Kolokotroni, M, Kotopouleas, A, Watkins, R, Giridharan, R and **Nikolopoulou, M.** 2022. Impact of reflective materials on urban canyon albedo, outdoor and indoor microclimates. *Building and Environment,* 207: 108459. DOI: https://doi.org/10.1016/j.buildenv.2021.108459

Salata, F, Golasi, I, Vollaro, ADL and **Vollaro, RDL.** 2015. How high albedo and traditional buildings' materials and vegetation affect the quality of urban microclimate. *A case study. Energy and Buildings,* 99: 32–49. DOI: https://doi.org/10.1016/j.enbuild.2015.04.010

Schrijvers, PJC, Jonker, HJJ, de Roode, SR and **Kenjereš S.** 2016. The effect of using a high-albedo material on the universal temperature climate index within a street canyon. *Urban Climate,* 17: 284–303. DOI: https://doi.org/10.1016/j.uclim.2016.02.005

Sen, S, Roesler, J, Ruddell, B and **Middel, A.** 2019. Cool pavement strategies for urban heat island mitigation in suburban Phoenix, Arizona. *Sustainability,* 11(16): Article 16. DOI: https://doi.org/10.3390/su11164452

Srivanit, M and **Jareemit, D.** 2020. Modeling the influences of layouts of residential townhouses and tree-planting patterns on outdoor thermal comfort in Bangkok suburb. *Journal of Building Engineering,* 101262. DOI: https://doi.org/10.1016/j.jobe.2020.101262

Steadman, RG. 1979. The assessment of sultriness. Part I: A temperature-humidity index based on human physiology and clothing science. *Journal of Applied Meteorology and Climatology,* 18(7): 861–873. DOI: https://doi.org/10.1175/1520-0450(1979)018<0861:TAOSPI>2.0.CO;2

Stone, B, Hess, JJ and **Frumkin, H.** 2010. Urban form and extreme heat events: are sprawling cities more vulnerable to climate change than compact cities? *Environmental Health Perspectives,* 118(10): 1425–1428. DOI: https://doi.org/10.1289/ehp.0901879

Takebayashi, H and **Moriyama, M.** 2012a. Relationships between the properties of an urban street canyon and its radiant environment: Introduction of appropriate urban heat island mitigation technologies. *Solar Energy* 86(9): 2255–2262. DOI: https://doi.org/10.1016/j.solener.2012.04.019

Takebayashi, H and **Moriyama, M.** 2012b. Study on surface heat budget of various pavements for urban heat island mitigation. *Advances in Materials Science and Engineering,* 2012: e523051. DOI: https://doi.org/10.1155/2012/523051

Taleghani, M. 2018. The impact of increasing urban surface albedo on outdoor summer thermal comfort within a university campus. *Urban Climate,* 24: 175–184. DOI: https://doi.org/10.1016/j.uclim.2018.03.001

Taleghani, M and **Berardi, U.** 2018. The effect of pavement characteristics on pedestrians' thermal comfort in Toronto. *Urban Climate,* 24: 449–459. DOI: https://doi.org/10.1016/j.uclim.2017.05.007

Taleghani, M, Kleerekoper, L, Tenpierik, M and **van den, Dobbelsteen, A.** 2015. Outdoor thermal comfort within five different urban forms in the Netherlands. *Building and Environment,* 83: 65–78. DOI: https://doi.org/10.1016/j.buildenv.2014.03.014

Thammapornpilas, J. 2015. Urban spatial development to mitigate urban heat island effect in the inner area of Bangkok. *Nakhara: Journal of Environmental Design and Planning,* 11: 29–40. https://ph01.tci-thaijo.org/index.php/nakhara/article/view/104849.

Tochaiwat, K, Rinchumphu, D, Sundaranaga, C, Pomsurin, N, Chaichana, C, Khuwuthyakorn, P, Phichetkunbodee, N and **Chan, YC.** 2023. The potential of a tree to increase comfort hours in campus public space design. *Energy Reports,* 9: 184–193. https://www.sciencedirect.com/science/article/pii/S2352484723010028. DOI: https://doi.org/10.1016/j.egyr.2023.05.258

US Department of Commerce. 2023. Heat Forecast Tools [Government Website]. National Weather Service; NOAA's National Weather Service [online access at https://www.weather.gov/safety/heat-index].

Vicedo-Cabrera, AM, Scovronick, N, Sera, F, Royé D, Schneider, R, Tobias, A, Astrom, C, Guo, Y, Honda, Y, Hondula, DM, Abrutzky, R, Tong, S, Coelho, MdeSZS, Saldiva, PHN, Lavigne, E, Correa, PM, Ortega, NV, Kan, H, Osorio, S, … Gasparrini, A. 2021. The burden of heat-related mortality attributable to recent human-induced climate change. *Nature Climate Change,* 11(6): Article 6. DOI: https://doi.org/10.1038/s41558-021-01058-x

Wongbumru, T and **Dewancker, B.** 2014. Public housing development and low-carbon society transitions: National housing authority's experiences and applications. *International Journal of Building, Urban, Interior and Landscape Technology (BUILT),* 4: 37–50. DOI: https://doi.org/10.56261/built.v4.170257

Yang, X and **Li, Y.** 2015. The impact of building density and building height heterogeneity on average urban albedo and street surface temperature. *Building and Environment,* 90: 146–156. DOI: https://doi.org/10.1016/j.buildenv.2015.03.037

Zhang, Y, Wei, P, Wang, L and **Qin, Y.** 2021. Temperature of paved streets in urban mockups and its implication of reflective cool pavements. *Atmosphere,* 12(5): Article 5. DOI: https://doi.org/10.3390/atmos12050560

Zhang, H, Yao, R, Luo, Q and **Wang, W.** 2022. A mathematical model for a rapid calculation of the urban canyon albedo and its applications. *Renewable Energy,* 197: 836–851. DOI: https://doi.org/10.1016/j.renene.2022.07.110

Zhao, M, Cai, H, Qiao, Z and **Xu, X.** 2016. Influence of urban expansion on the urban heat island effect in Shanghai. *International Journal of Geographical Information Science,* 30(12): 2421–2441. DOI: https://doi.org/10.1080/13658816.2016.1178389

Zheng, T, Qu, K, Darkwa, J and **Calautit, JK.** 2022. Evaluating urban heat island mitigation strategies for a subtropical city centre (a case study in Osaka, Japan). *Energy,* 250: 123721. DOI: https://doi.org/10.1016/j.energy.2022.123721